

We are IntechOpen, the world's leading publisher of Open Access books Built by scientists, for scientists

6,900

Open access books available

185,000

International authors and editors

200M

Downloads

Our authors are among the

154

Countries delivered to

TOP 1%

most cited scientists

12.2%

Contributors from top 500 universities



WEB OF SCIENCE™

Selection of our books indexed in the Book Citation Index
in Web of Science™ Core Collection (BKCI)

Interested in publishing with us?
Contact book.department@intechopen.com

Numbers displayed above are based on latest data collected.
For more information visit www.intechopen.com



Adaptive Heterodyne Filters

Michael A. Soderstrand
University of California (Retired)
Department of Electrical and Computer Engineering,
Oklahoma State University (Retired)
Washington, D.C.
United States of America

1. Introduction

The heterodyne process has been an important part of electronic communications systems for over 100 years. The most common use of the heterodyne process is in modulation and demodulation where a local oscillator produces the heterodyne signal which is then mixed with (multiplied by) the signal of interest to move it from one frequency band to another. For example, the superheterodyne receiver invented by U.S. Army Major Edwin Armstrong in 1918 uses a local oscillator to move the incoming radio signal to an intermediate band where it can be easily demodulated with fixed filters rather than needing a variable filter or series of fixed filters for each frequency being demodulated (Butler, 1989, Duman 2005). Today you will find heterodyne as a critical part of any modern radio or TV receiver, cell phone, satellite communication system, etc.

In this chapter we will introduce the concept of making a tunable or adaptive filter using the heterodyne process. The concept is very similar to that of the superheterodyne receiver, but applied to tunable filters. Most tunable filters require a complicated mechanism for adjusting the coefficients of the filter in order to tune the filter. Using the heterodyne approach, we move the signal to a fixed filter and then move the signal back to its original frequency band minus the noise that has been removed by the fixed filter. Thus complicated fixed filters that would be virtually impossible to tune using variation of the filter parameters can be easily made tuneable and adaptive.

1.1 Applications of adaptive heterodyne filters

Modern broad-band wireless systems are designed to be co-located with older narrow-band communications so as to be able to share valuable spectrum (Etkin et al., 2005, Peha, 1998, 2000). This is accomplished by using a pseudorandom number sequence to control the spreading of the spectrum of the modern wireless transmitter so that it appears to be background noise that is easily filtered out by the narrow-band receiver. The five most common techniques for achieving spread-spectrum communications are (1) Frequency Hopping Spread Spectrum (FHSS, e.g.: IEEE 802.11-1997) in which the signal is transmitted at a random series of frequencies across the spectrum, (2) Direct Sequence Spread Spectrum (DSSS, e.g.: IEEE 802.11b and 802.11g) in which the transmitter multiplies the signal by a random sequence to make it appear like background noise, (3) Time Hopping Spread

Spectrum (THSS, e.g.: IEEE 802.15) in which the carrier is turned on and off by the random code sequence, (4) Chirp Spread Spectrum (CSS, e.g.: IEEE 802.15.4a-2007) which uses wideband linear frequency modulated chirp pulses to encode the information, and (5) Ultra Wide Band (UWB, e.g.: IEEE 802.15.3a - Note: No standard assigned, MB-OFDM and DS-UWB will compete in market) based on transmitting short duration pulses.

When working properly, the narrow-band transmissions licensed to the frequency spectrum do not affect the broadband systems. They either interfere with a small portion of the broadband transmission (which may be re-sent or reconstructed) or the narrow-band signals are themselves spread by the receiver demodulation process (Pickholtz et al., 1982). However, in practice the narrow-band transmissions can cause serious problems in the spread-spectrum receiver (Coulson, 2004, McCune, 2000). To alleviate these problems, it is often necessary to include narrow-band interference attenuation or suppression circuitry in the design of the spread-spectrum receiver. Adaptive heterodyne filters are an attractive approach for attenuation of narrow-band interference in such broadband systems. Other approaches include smart antennas and adaptive analog and digital filters, but adaptive heterodyne filters are often a good choice for attenuation of narrow band interference in broadband receivers (Soderstrand, 2010a).

1.2 Preliminary concepts

Figure 1 shows the most common digital heterodyne circuit. The incoming signal $x(n)$ is multiplied by the heterodyne signal $\cos(\omega_0 n)$. The parameter ω_0 is the heterodyne frequency which, along with all frequencies contained in $x(n)$, must be less than $\pi/2$ in order to avoid aliasing.

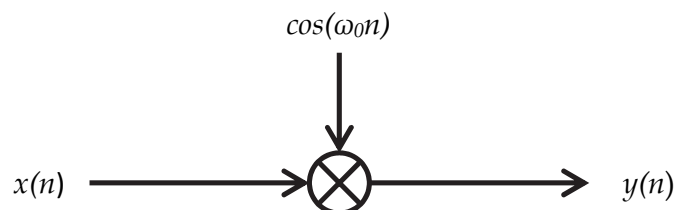


Fig. 1. Basic digital heterodyne operation.

Most textbooks analyze this basic heterodyne operation in the time domain making use of trigonometric identities to show that the effect of the heterodyne operation is to generate two images of the input signal $x(n)$, one translated up in frequency by ω_0 and the other translated down in frequency by ω_0 . However, for our purposes it is better to view things in the frequency domain (z -domain).

The time domain multiplication of $x(n)$ by $e^{j\omega_0 n}$ rotates the z -domain representation of the signal $X(z)$ left by ω_0 to $X(ze^{-j\omega_0})$. The signal that was at DC, now appears at $-\omega_0$. Similarly, the time domain multiplication of $x(n)$ by $e^{-j\omega_0 n}$ rotates the z -domain representation of the signal $X(z)$ right by ω_0 to $X(ze^{j\omega_0})$. The signal that was at DC, now appears at ω_0 . This important relationship is expressed in the following equation (Dorf & Wan, 2000, Roberts, 2007):

$$x(n)e^{j\omega_0 n} \stackrel{Z}{\Leftrightarrow} X(ze^{-j\omega_0}) \quad (1)$$

If we express $\cos(\omega_0 n)$ in terms of the complex exponential, we get the following:

$$x(n) \cos(\omega_0 n) = \frac{1}{2} x(n) [e^{j\omega_0 n} + e^{-j\omega_0 n}] \stackrel{Z}{\Leftrightarrow} \frac{1}{2} [X(ze^{-j\omega_0}) + X(ze^{j\omega_0})] \quad (2)$$

From equation (2) we can clearly see the separation of the input signal into two signals, one translated in frequency by rotation to the left ω_0 and the other translated in frequency by rotation to the right ω_0 in the z -plane. In a modulation system, we would filter out the lower frequency and send the higher frequency to the antenna for transmission. In a demodulator, we would filter out the higher frequency and send the lower frequency to the IF stage for detection.

1.3 A simple tunable heterodyne band-pass filter

The basic heterodyne operation of Figure 1 can be used to implement a simple tunable narrow-band band-pass filter using the circuit of Figure 2.

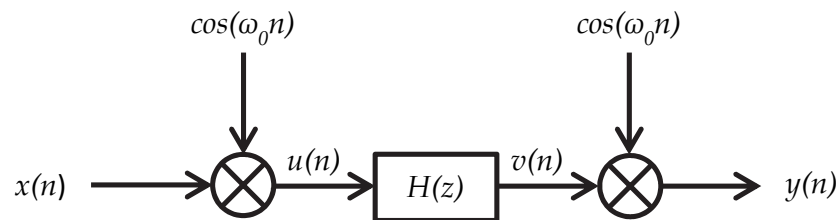


Fig 2. Simple tunable heterodyne band-pass filter ($H(z)$ must be a narrow-band low-pass filter)

Using the same analysis as equation (2) we obtain:

$$u(n) = x(n) \cos(\omega_0 n) = \frac{1}{2} x(n) [e^{j\omega_0 n} + e^{-j\omega_0 n}] \stackrel{Z}{\Leftrightarrow} U(z) = \frac{1}{2} [X(ze^{-j\omega_0}) + X(ze^{j\omega_0})] \quad (3)$$

After the filter stage we have:

$$V(z) = \frac{1}{2} [X(ze^{-j\omega_0}) + X(ze^{j\omega_0})] H(z) \quad (4)$$

The final heterodyne operation then results in the output $Y(z)$:

$$Y(z) = \frac{1}{4} [H(ze^{-j\omega_0}) + H(ze^{j\omega_0})] X(z) + \frac{1}{4} [H(ze^{-j\omega_0}) X(ze^{-2j\omega_0}) + H(ze^{j\omega_0}) X(ze^{2j\omega_0})] \quad (5)$$

Equation (5) is obtained by the straight-forward application of equation (1) for the multiplication of equation (4) by the cosine heterodyne function. Equation (5) consists of four separate terms. If $H(z)$ is a narrow-band low-pass filter, then the first two terms of equation (5) represent a narrow-band band-pass filter centered at the heterodyne frequency ω_0 .

$$Y_{BP}(z) = \frac{1}{4} [H(ze^{-j\omega_0}) + H(ze^{j\omega_0})] X(z) \quad (6)$$

This narrow-band band-pass filter has only half the energy, however, because the other half of the energy appears in the high-frequency last terms in equation (5).

$$Y_{HF}(z) = \frac{1}{4} [H(ze^{-j\omega_0}) X(ze^{-2j\omega_0}) + H(ze^{j\omega_0}) X(ze^{2j\omega_0})] \quad (7)$$

However, if $H(z)$ is of sufficiently narrow bandwidth, these high-frequency terms will be attenuated by $H(z)$ and equation (6) will substantially represent the output of the simple tunable heterodyne filter of Figure 2.

Figure 3 shows the impulse response of the circuit of Figure 1 as simulated in MatLab for four different values of the heterodyne frequency. Figure 3 was implemented by the following MatLab script (COSHET):

```
% COSHET (Lab book p. 129 12/11/2010)
% Function to implement cosine heterodye filter
% Set the following inputs before calling COSHET:
%     inp = 0 (provide input file inpf)
%         = 1 (impulse response)
%     npoints = number of points in input
%     w0 = heterodyne frequency
%     [b a] = coefficients of filter H(z)
%
% OUTPUTS: hdb = frequency response of the filter
if inp==1
    for index=1:npoints
        inpf(index)=0;
    end
    inpf(1)=1;
end
for index=1:npoints
    x(index)=inpf(index)*sqrt(2)*cos(w0*(index-1));
end
y=filter(b,a,x);
for index=1:npoints
    yout(index)=y(index)*sqrt(2)*cos(w0*(index-1));
end
h=fft(yout);
hdb=20*log10(abs(h));
plot(hdb,'k')
```

Before invoking the above script each of the input values was set ($\text{inp}=1$, $\text{npoints}=1000$, $\omega_0 = \pi/5$, $\omega_0 = 2\pi/5$, $\omega_0 = 3\pi/5$ and $\omega_0 = 4\pi/5$). The filter $H(z)$ was selected as an inverse-Chebyshev filter designed as $[b,a] = \text{cheby2}(11, 40, 0.1)$. As can be seen from Figure 3, we have been able to implement a tunable narrow-band band-pass filter that can be tuned by the changing the heterodyne frequency.

Figure 4 shows a MatLab simulation of the ability of the circuit of Figure 2 to attenuate frequencies outside the band-pass filter and pass frequencies inside the bandwidth of the band-pass filter. The following MatLab script (GENINP) generates an input signal consisting of nine cosine waves spaced by $\pi/10$ in the z -plane:

```

% GENINP (Lab book p. 129 12/11/2010)
% Generates nine sinusoidal inputs spaced by pi/10
% INPUTS: npoints = number of points
for index=1:npoints
    inpf(index)=cos(pi*(index-1)/10);
    inpf(index)=inpf(index)+cos(2*pi*(index-1)/10);
    inpf(index)=inpf(index)+cos(3*pi*(index-1)/10);
    inpf(index)=inpf(index)+cos(4*pi*(index-1)/10);
    inpf(index)=inpf(index)+cos(5*pi*(index-1)/10);
    inpf(index)=inpf(index)+cos(6*pi*(index-1)/10);
    inpf(index)=inpf(index)+cos(7*pi*(index-1)/10);
    inpf(index)=inpf(index)+cos(8*pi*(index-1)/10);
    inpf(index)=inpf(index)+cos(9*pi*(index-1)/10);
end

```

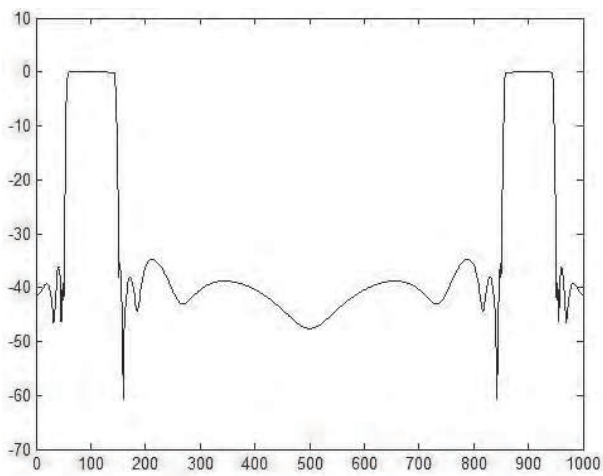
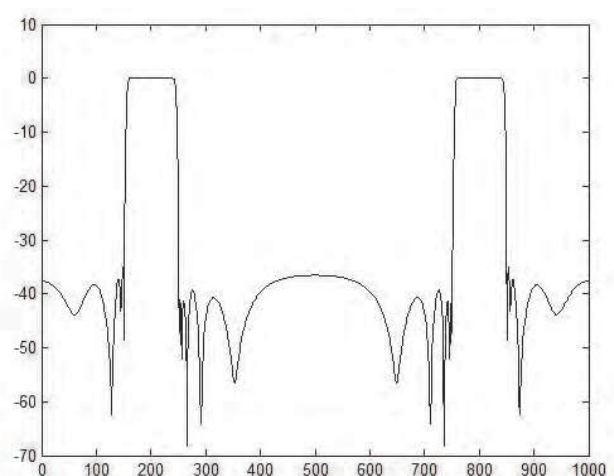
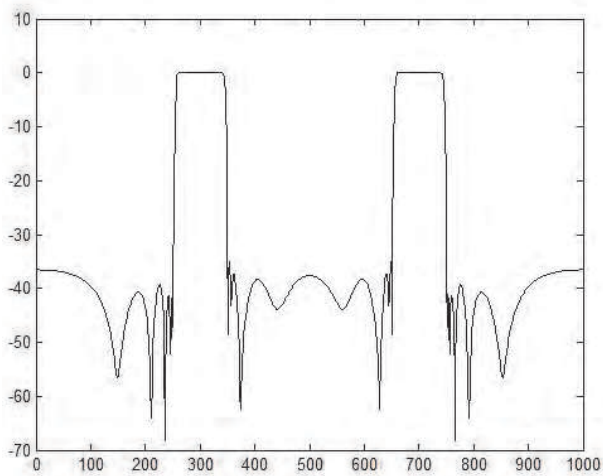
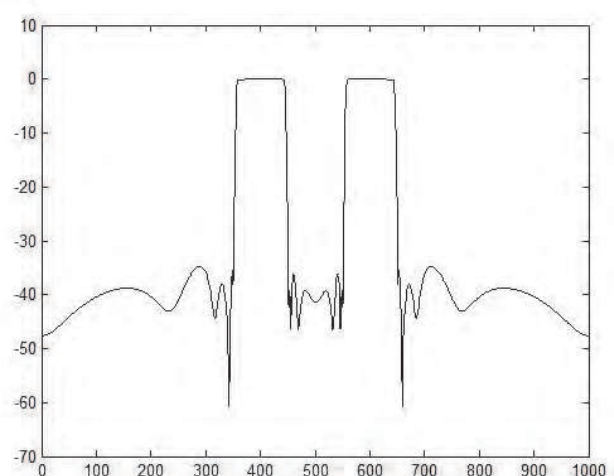
Fig. 3a. Tunable band-pass filter with $\omega_0 = \pi/5$ Fig. 3b. Tunable band-pass filter with $\omega_0 = 2\pi/5$ Fig. 3c. Tunable band-pass filter with $\omega_0 = 4\pi/5$ Fig. 3d. Tunable band-pass filter with $\omega_0 = 4\pi/5$

Fig. 3. MatLab simulation of circuit of Figure 2 for various values of the heterodyne frequency ω_0 .

This input is then used with the previous script (COSHET) to generate Figure 4 (inp=0).

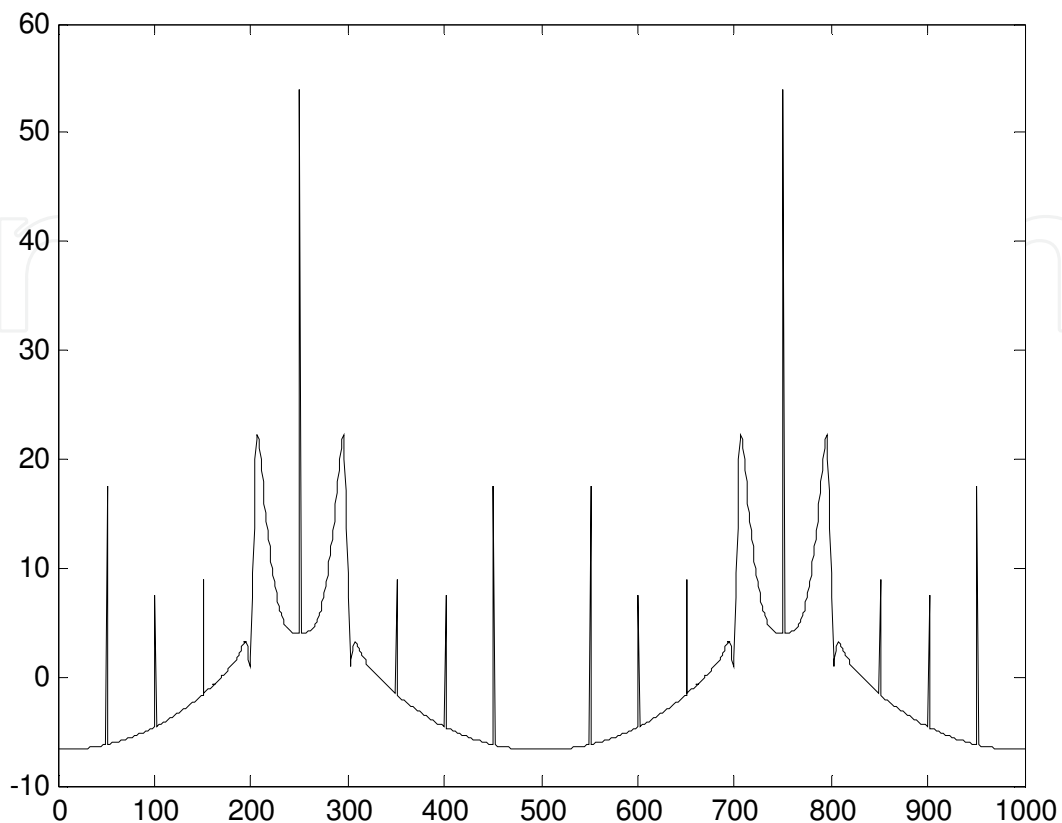


Fig. 4. Output of circuit of figure 2 when input is nine equally-spaced cosine waves.

In Figure 4 you can see the nine equally spaced cosine waves. The heterodyne frequency was set to $\pi/2$. Thus the cosine waves at all frequencies except $\pi/2$ are severely attenuated. There is nearly 40db difference between the cosine output at $\pi/2$ and the cosine output at other frequencies. Once again, this verifies the ability of the circuit of Figure 2 to implement a tunable narrow-band band-pass filter. (NOTE: The plots obtained from MatLab label the Nyquist frequency π as 500. The plots show the entire frequency response from 0 to 2π . Hence, the cosine at $\pi/2$ appears at 250 on the x-axis.)

1.4 Problems with the simple tunable heterodyne structure

While the Simple Tunable Heterodyne Band-Pass Filter of Section 1.3 works very well, attempts to use the structure of Figure 2 to realize tunable wide-band filters such as tunable Band-Stop or Notch Filters, tunable cut-off frequency Low Pass or High Pass Filters or tunable bandwidth Band-Pass Filters will fail. Equation (7) represents the high-frequency components at $2\omega_0$ that must be substantially attenuated by $H(z)$ in order to prevent interference with the desired filter of equation (6). In the case of a wide-band $H(z)$, this attenuation does not happen and interference destroys the operation of the filter.

But an even more serious problem is in equation (6) itself. For example, if we try to design a tunable Band-Stop Filter by making $H(z)$ a wide-band High-Pass Filter, equation (6) indicates that the stop-band of the High-Pass Filter $H(z)$ has been moved to $\pm\omega_0$ as desired to attenuate frequencies around $\pm\omega_0$. However, since $H(z)$ passes frequencies away from $\pm\omega_0$,

the maximum attenuation that can be achieved across the stop band is only 6db! This is illustrated in Figure 5 where we have replaced the narrow-band band-pass $H(z)$ from the previous section with a wide-band high-pass $H(z)$.

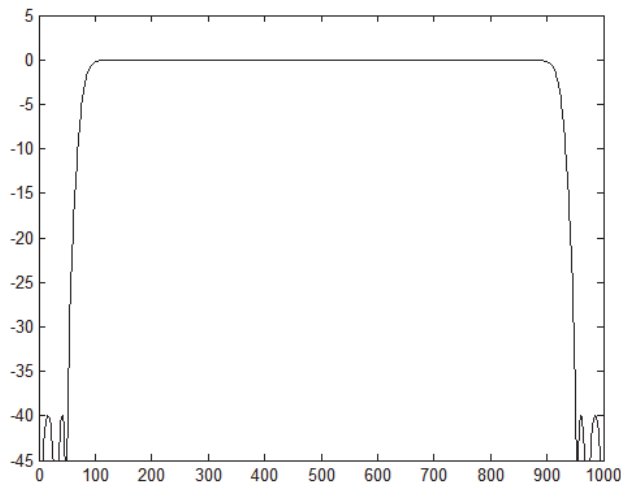


Fig. 5a. $H(z)$ for a wideband high-pass filter

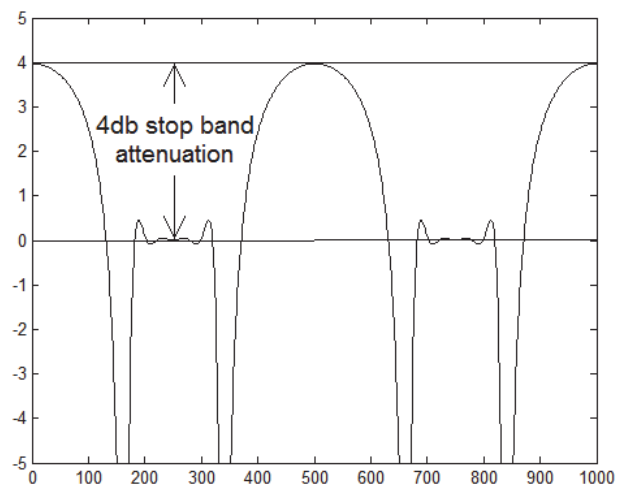


Fig. 5b. Tunable band-stop filter
(poor attenuation)

Fig. 5. Demonstration of failure of circuit 2 to work with wide-band functions.

2. The complex digital heterodyne circuit

The key to designing Complex Heterodyne Tunable Filters is in the modification of the Basic Digital Heterodyne Circuit of Figure 1 into the Complex Digital Heterodyne Circuit shown in Figure 6a. When implemented in software or in hardware that supports complex arithmetic, the circuit is of little more complexity than the Basic Digital Heterodyne circuit of Figure 1. However, in standard hardware we must implement the complex arithmetic using standard digital hardware as shown in Figure 6b. Figure 6b is the complete implementation of the Complex Digital Heterodyne Circuit of Figure 6a. Figures 6c and 6d show simplified hardware for real input and for real output respectively. In the remainder of this chapter, we shall use the circuit diagram of Figure 6a to represent all the circuits of Figure 6.

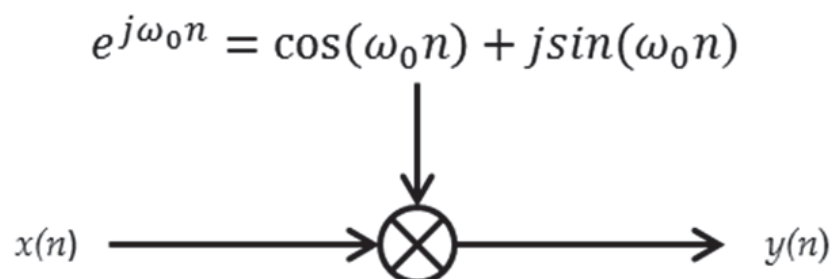


Fig. 6a. Complex heterodyne circuit for software or hardware that supports complex arithmetic

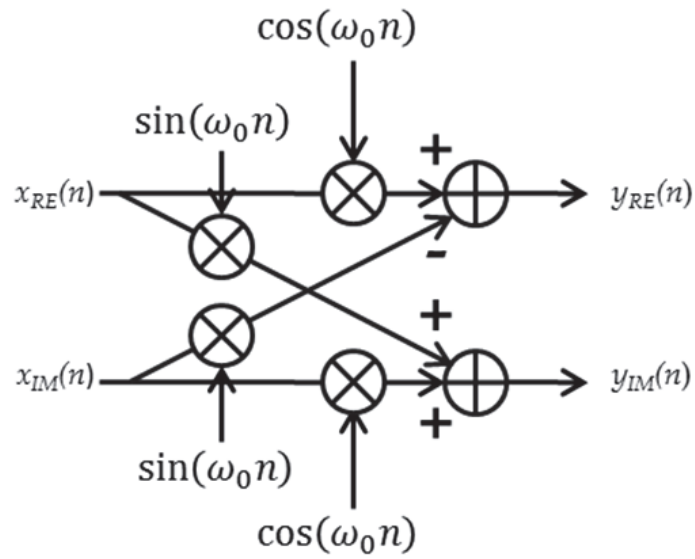


Fig. 6b. Complete hardware implementation of complex digital heterodyne circuit.

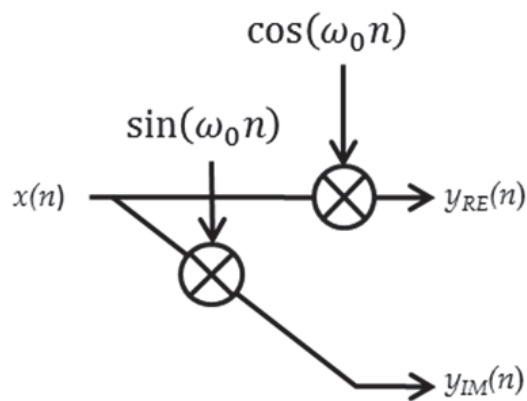


Fig. 6c. Implementation of real-input complex digital heterodyne

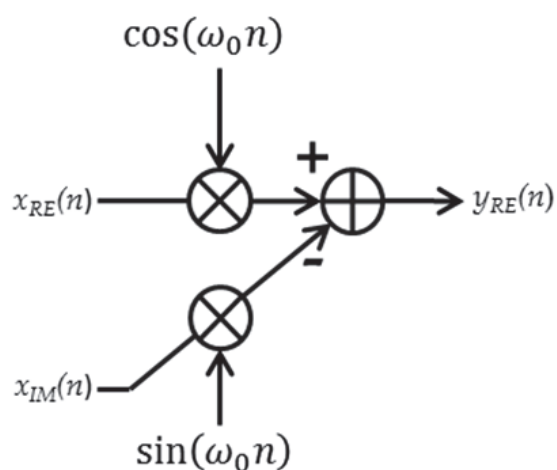


Fig. 6d. Implementation of real-output complex digital heterodyne.

Fig. 6. Implementations of the complex heterodyne circuit

2.1 Complex heterodyne rotation

Now we consider what happens when we replace the basic digital heterodyne circuit in Figure 2 with the complex digital heterodyne unit of Figure 6 to obtain the Complex Heterodyne Rotation Circuit of Figure 7.

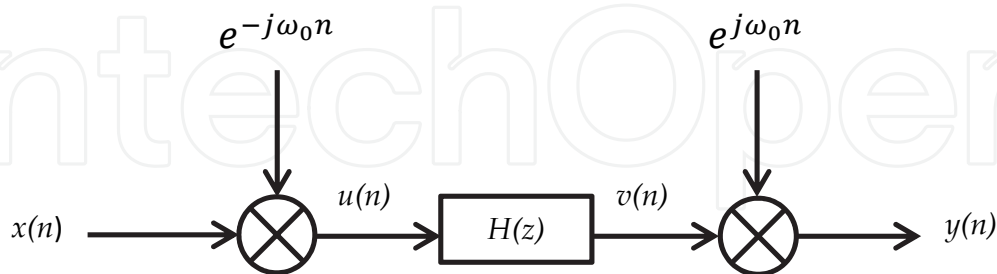


Fig. 7. Complex heterodyne rotation circuit (Rotates $H(z)$ by ω_0 in the z -plane so that what was at DC is now at ω_0)

The MatLab code to implement Figure 7 is as follows:

```
% EXPHET (Lab book p. 129 12/11/2010)
% Function to implement complex exponential heterodyne
% filter
% Set the following inputs before calling EXPHET:
%   inp = 0 (provide input file inpf)
%   = 1 (impulse response)
%   npoints = number of points in input
%   w0 = heterodyne frequency
%   [b a] = coefficients of filter H(z)
% OUTPUTS: hdb = frequency response of the filter
clear x y yout hdb
if inp==1
    for index=1:npoints
        inpf(index)=0;
    end
    inpf(1)=1;
end
for index=1:npoints
    x(index)=inpf(index)*exp(-1i*w0*(index-1));
end
y=filter(b,a,x);
for index=1:npoints
    yout(index)=y(index)*exp(1i*w0*(index-1));
end
hdb=20*log10(abs(fft(yout)));
plot(hdb,'k')
```

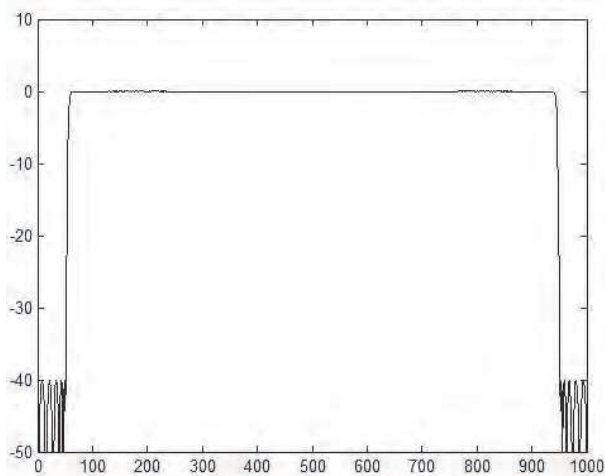


Fig. 8a. Frequency response of prototype filter

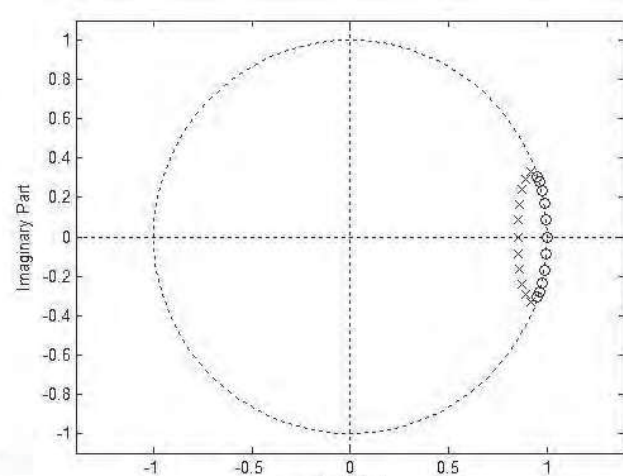


Fig. 8b. Pole-zero plot of prototype filter

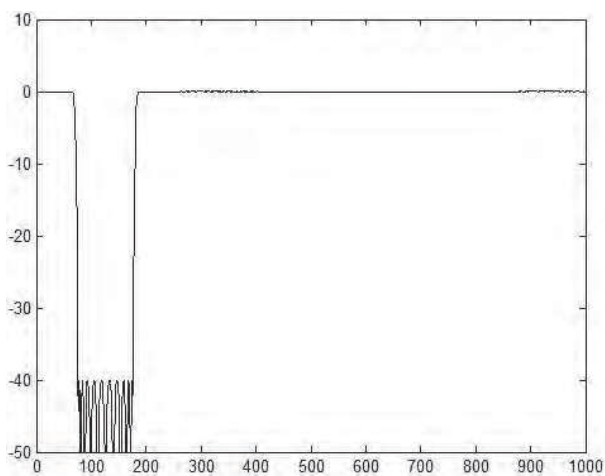


Fig. 8c. Frequency response of rotated filter

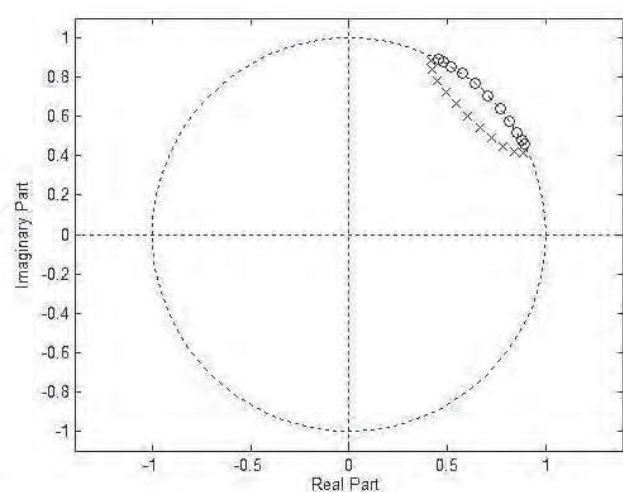


Fig. 8d. Pole-zero plot of rotated filter

Fig. 8. Demonstration of complex heterodyne rotation circuit of Figure 7

Using the same prototype wideband High-Pass Filter as we used in Section 1.4 to get Figures 5a and 5b, let's use this prototype filter in the Complex Heterodyne Rotation Circuit of Figure 7. The results are shown in Figure 8. Figure 8a shows the frequency response of the prototype wideband High-Pass Filter, Figure 8b shows the pole-zero plot for this prototype filter, Figure 8c shows the frequency response of the rotated filter at the output of Figure 7, and Figure 8d shows the pole-zero plot for the circuit of Figure 7 with the wideband High-Pass prototype filter used for $H(z)$.

Figure 8 demonstrates the ability of the Complex Heterodyne Rotation Circuit of Figure 7 to rotate poles and zeros in the z -plane. However, the output of Figure 7 is not real. It is a complex output generating a frequency response that is not symmetric around the Nyquist frequency. This means that the filter will attenuate frequencies at $+\omega_0$ but not at $-\omega_0$. Since real systems have frequencies at both $+\omega_0$ and $-\omega_0$, the circuit of Figure 7 cannot be used to implement a band-stop filter for real systems. In sections 3, 4 and 5 we shall see three different ways we can make use of the basic circuit of Figure 7 to implement tunable band-stop and notch filters, tunable cut-off frequency high-pass and low-pass filters, and tunable bandwidth band-pass filters.

3. Three-way tunable complex heterodyne filter (Azam's technique)

The basic structure for Tunable Complex Heterodyne filters is shown in Figure 9. This Three-Way Tunable Complex Heterodyne circuit consists of three complex heterodyne units of Figure 6 and two identical prototype filters $H(z)$. By selecting the correct prototype filter, we are able to design tunable band-stop and notch filters, tunable cut-off frequency low-pass and high-pass filters and tunable bandwidth band-pass and band-stop filters. These filters are maximally tunable in that the band-pass and band-stop filters can be tuned from DC to the Nyquist frequency and the other filters can be tuned such that their bandwidth varies from zero to half the Nyquist frequency. There is no distortion in the filters, the prototype design transfers directly except that the pass-band ripple is doubled, thus we must design prototype filters with half the desired pass-band ripple.

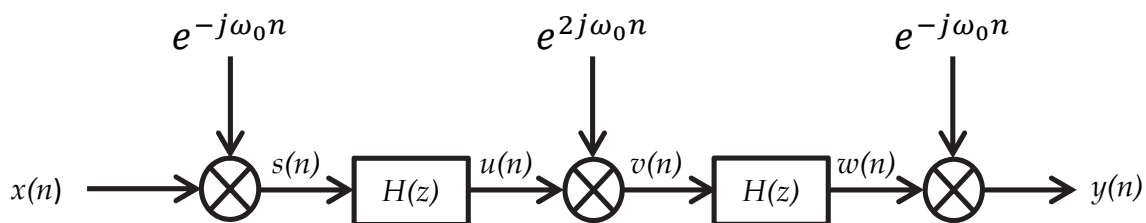


Fig. 9. Three-way tunable complex heterodyne filter (Azam's method)



Fig. 10a. Input $X(z)$ Fig. 10b. Rotate ω_0 to DC Fig. 10c. Rotate $-\omega_0$ to DC Fig. 10d. Rotate back

Fig. 10. Creation of a notch at $\pm\omega_0$ using the three-way tunable complex heterodyne filter of Figure 9 (z-plane).

Before we look at the detailed analysis of Figure 9, let's take an overview of its operation. In order to make the procedure clear, let's assume that $H(z)$ is a wide-band high-pass filter like that of Figure 8a and 8b. Then the first heterodyne operation rotates the input signal $x(n)$ (shown in Figure 10a.) by $-\omega_0$ so that the frequencies that were at DC are now located at $-\omega_0$ (see Figure 10b). $H(z)$ is then applied attenuating frequencies that were at ω_0 in $x(n)$ before the rotation (indicated by white spot in Figure 10b). At this point if we simply rotated back like we did in the circuit of Figure 7, we would get the rotated $H(z)$ as shown in Figure 8c and 8d. However, in Figure 9 we now rotate back $2\omega_0$ so that the frequencies of $x(n)$ that were at DC are now at $+\omega_0$ in $x(n)$ (see Figure 10c). The second identical $H(z)$ then attenuates frequencies in $x(n)$ that were at $-\omega_0$ before any of these rotations (indicated by second white spot in Figure 10c). Finally, we rotate the signal back to its original frequencies with the attenuation having been applied both at $+\omega_0$ (first $H(z)$) and $-\omega_0$ (second $H(z)$) as shown in Figure 10d. Since $H(z)$ is applied twice, we will experience twice the pass-band ripple. Hence, the prototype filter $H(z)$ must be designed with one-half the ripple desired in the

final filter. Also because $H(z)$ is applied twice, some portions of the stop-band will have twice the attenuation while other parts will have the desired attenuation. Having more attenuation than specified is not a problem, so we will design the prototype filter $H(z)$ with the desired stop-band attenuation (not half the stop-band attenuation).

Now let's look at the detailed mathematics of Figure 9. Making use of the relationship of Equation 1, we have the following as a result of passing $x(n)$ (see Figure 10a) through the first complex heterodyne unit in Figure 9:

$$x(n)e^{-j\omega_0 n} \stackrel{Z}{\Leftrightarrow} X(ze^{j\omega_0}) \quad (8)$$

Next we apply the prototype filter $H(z)$ (see Figure 10b):

$$x(n)e^{-j\omega_0 n} * h(n) \stackrel{Z}{\Leftrightarrow} X(ze^{j\omega_0})H(z) \quad (9)$$

Now we rotate back $2\omega_0$ by passing through the second complex heterodyne unit (see Figure 10c):

$$[x(n)e^{-j\omega_0 n} * h(n)]e^{2j\omega_0 n} \stackrel{Z}{\Leftrightarrow} X(ze^{-j\omega_0})H(ze^{-2j\omega_0 n}) \quad (10)$$

We then apply the second identical prototype filter $H(z)$ (see Figure 10c):

$$\{[x(n)e^{-j\omega_0 n} * h(n)]e^{2j\omega_0 n}\} * h(n) \stackrel{Z}{\Leftrightarrow} X(ze^{-j\omega_0})H(ze^{-2j\omega_0 n})H(z) \quad (11)$$

Finally we pass through the last complex heterodyne unit returning the signal to its original location (see Figure 10d):

$$(\{[x(n)e^{-j\omega_0 n} * h(n)]e^{2j\omega_0 n}\} * h(n))e^{-j\omega_0 n} \stackrel{Z}{\Leftrightarrow} X(z)H(ze^{-j\omega_0 n})H(ze^{j\omega_0 n}) \quad (12)$$

The transfer function shown in equation (12) above is the effect of the entire Three-Way Tunable Complex Heterodyne Filter shown in Figure 9. By choosing different prototype filters $H(z)$ we are able to implement tunable center-frequency band-stop and notch filters, tunable cut-off frequency low-pass and high-pass filters, and tunable bandwidth band-pass and band-stop filters. In the following sections we will look at the details for each of these designs.

Designing tunable filters using the Three-Way Complex Heterodyne circuit of Figure 9 is simply a matter of choosing the correct prototype filter $H(z)$. Table 1 on the next page shows the types of tunable filters that can be designed using the Three-Way Complex Heterodyne Technique including the requirements for the prototype filter $H(z)$ and the tunable range. In the following sections we shall make use of this table to design examples of each of these tunable filters.

3.1 Design of tunable center-frequency band-stop filter

In this and the following five sections we will give an example of each of the filter designs in Table 1. In all of these designs the prototype filter $H(z)$ may be designed using any of the many filter design techniques. For example, in MatLab we may design Butterworth (`butter`), Chebyshev (`cheby1`), inverse Chebyshev (`cheby2`), elliptical (`ellip`) or Parks-McClellan Linear Phase Filters (`firpm`) to name a few. The Three-Way Complex Heterodyne Circuit of Figure 9 and Table 1 will preserve the key characteristics of the prototype filter except as

noted in Table 1. The examples in this chapter will all be based on linear-phase Parks-McClellan filters. The prototype filter $H(z)$ will use a 64-tap prototype filter with weights designed to obtain 40db attenuation in the stop band and a maximum ripple of 1.5db in the prototype filter pass-band (3db in the tunable filter pass-band).

Desired Tunable Filter	Required $H(z)$	Tunable Range
Tunable center-frequency band-stop filter	High-pass filter with cut-off frequency equal to one-half of the desired band-width, pass-band ripple equal to one-half the desired pass-band ripple and stop-band attenuation equal to the desired stop-band attenuation for the tunable center-frequency band-stop filter.	Fully tunable from DC to the Nyquist frequency.
Tunable cut-off frequency low-pass filter	Low-pass filter with cut-off frequency equal to one-half of the Nyquist frequency, pass-band ripple equal to one-half the desired pass-band ripple and stop-band attenuation equal to the desired stop-band attenuation for the tunable cut-off frequency low-pass filter.	Cut-off frequency tunable from DC to one-half the Nyquist frequency
Tunable cut-off high-pass filter	High-pass filter with cut-off frequency equal to one-half of the Nyquist frequency, pass-band ripple equal to one-half the desired pass-band ripple and stop-band attenuation equal to the desired stop-band attenuation for the tunable cut-off frequency high-pass filter.	Cut-off frequency tunable from DC to one-half the Nyquist frequency
Tunable band-width band-pass filter	Band-pass filter centered at $\pi/2$ with band-width of $\pi/2$, pass-band ripple equal to one-half the desired pass-band ripple and stop-band attenuation equal to the desired stop-band attenuation for the tunable band-width band-pass filter.	Bandwidth tunable from Δ to $\pi/2$
Tunable band-width band-stop filter	Band-stop filter centered at $\pi/2$ with band-width of $\pi/2$, pass-band ripple equal to one-half the desired pass-band ripple and stop-band attenuation equal to the desired stop-band attenuation for the tunable band-width band-stop filter.	Bandwidth tunable from Δ to $\pi/2$
NOTE: In bandwidth tuning, Δ is the smallest bandwidth available. The actual value of Δ depends on the transition band of the prototype filter $H(z)$. The narrower the transition band, the smaller the value of Δ . Attempts to tune the bandwidth to less than Δ will result in leakage at DC and the Nyquist frequency.		

Table 1. Design of tunable filters using the three-way complex heterodyne circuit of Figure 9

The following MatLab code is used to implement the Three-Way Complex Heterodyne Circuit of Figure 9:

```

% N3WAYHET
% Implements the Three-Way Heterodyne Rotation Filter
% Also known as the Full-Tunable Digital Heterodyne Filter
% INPUTS:
% Set the following inputs before calling 3WAYHET:
%   inp = 0 (provide input file inpf)
%   inp = 1 (impulse response)
%   npoints = number of points in input
%   w0 = heterodyne frequency
%   [b a] = coefficients of filter H(z)
%   scale = 0 (do not scale the output)
%   scale = 1 (scale the output to zero db)
%
% OUTPUTS: ydb = frequency response of the filter
%          hdb, sdb, udb, vdb, wdb (intermediate outputs)
clear y ydb hdb s sdb u udb v vdb w wdb
if inp==1
    for index=1:npoints
        inpf(index)=0;
    end
    inpf(1)=1;
end
for index=1:npoints
    s(index)=inpf(index)*exp(-1i*w0*(index-1));
end
u=filter(b,a,s);
for index=1:npoints
    v(index)=u(index)*exp(+2*1i*w0*(index-1));
end
w=filter(b,a,v);
for index=1:npoints
    y(index)=w(index)*exp(-1i*w0*(index-1));
end
[h,f]=freqz(b,a,npoints,'whole');
hdb=20*log10(abs(h));
sdb=20*log10(abs(fft(s)));
udb=20*log10(abs(fft(u)));
vdb=20*log10(abs(fft(v)));
wdb=20*log10(abs(fft(w)));
ydb=20*log10(abs(fft(y)));
if scale==1
    ydbmax=max(ydb)
    ydb=ydb-ydbmax;
end
plot(ydb,'k')

```

To design a tunable center-frequency band-pass filter, the prototype filter must be a narrow-band low-pass filter with the bandwidth equal to half the bandwidth of the desired tunable band-pass filter. Before calling the MatLab m-file `n3wayhet`, we initialize the input variables as follows:

```
inp=1;npoints=1000;w0=0;a=1;b=firpm(64,[0 .1*.8 .1/.8 1],[0 0 1 1],[10 1]);scale=1 n3wayhet;
```

Figure 11 shows the design criteria for the prototype wide-band high-pass filter needed to implement the tunable band-stop filter. The prototype high-pass filter needs a stop-band bandwidth of one-half the desired bandwidth of the tunable notch filter. The prototype filter must have one-half the pass-band ripple of the desired pass-band ripple for the tunable band-pass filter. However, the prototype high-pass filter should have the same stop-band attenuation as is desired in the tunable band-stop filter.

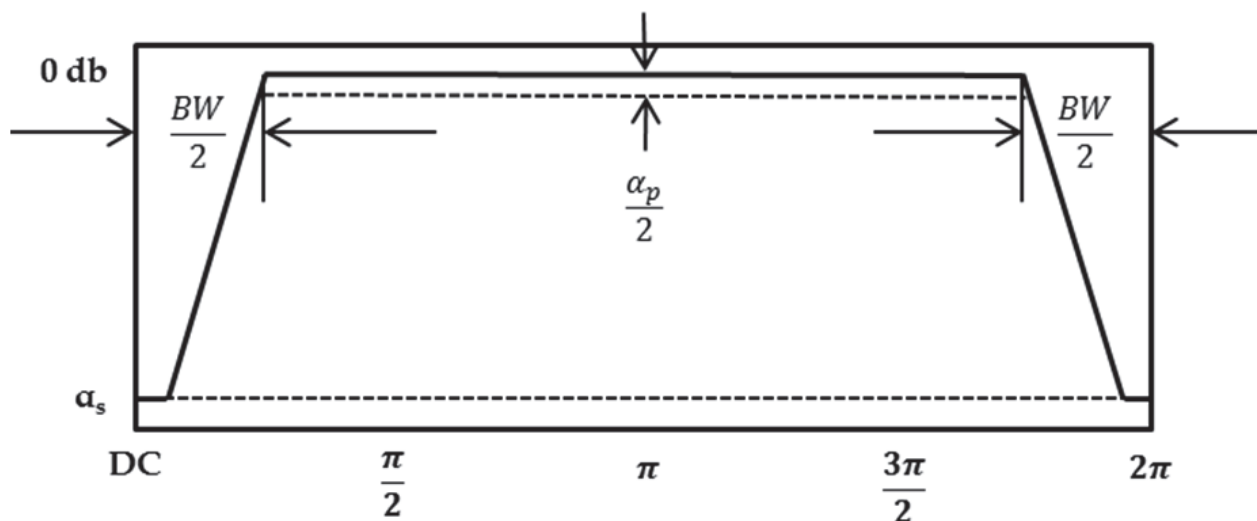


Fig. 11. Design criteria for prototype wide-band high-pass filter $H(z)$ required to implement a tunable band-stop filter using the three-way complex heterodyne circuit of Figure 9.

Figure 12 shows the result of running this MatLab m-file simulation of the circuit of Figure 9 for four different values of ω_0 , $\omega_0 = 0$, $\omega_0 = \frac{\pi}{4}$, $\omega_0 = \frac{\pi}{2}$ and $\omega_0 = \frac{3\pi}{4}$. Key features of the Three-Way Complex Heterodyne Technique can be seen in Figure 12. First, when $\omega_0 = 0$ we get the frequency response shown in Figure 12a which is the prototype filter convolved with itself ($H(z)H(z)$). Thus we have over 80db attenuation in the stop band and the desired less than 3db ripple in the pass-band. The prototype filter is High-Pass. Figure 12b shows the circuit with $\omega_0 = \pi/4$. This tunes the center frequency to $\pi/4$ which shows up as 125 on the x-axis of Figure 12b. Figure 12c shows the circuit with $\omega_0 = \pi/2$. This tunes the center frequency to $\pi/2$ which shows up as 250 on the x-axis of Figure 12c. Figure 12d shows the circuit with $\omega_0 = 3\pi/4$. This tunes the center frequency to $3\pi/4$ which shows up as 375 on the x-axis of Figure 12d. Notice that the attenuation of the tuned band-stop filters is over 40db which is the same stop-band attenuation as the prototype filter. All of these filters retain the linear-phase property of the prototype filter that was designed using the Parks-McClellan algorithm.

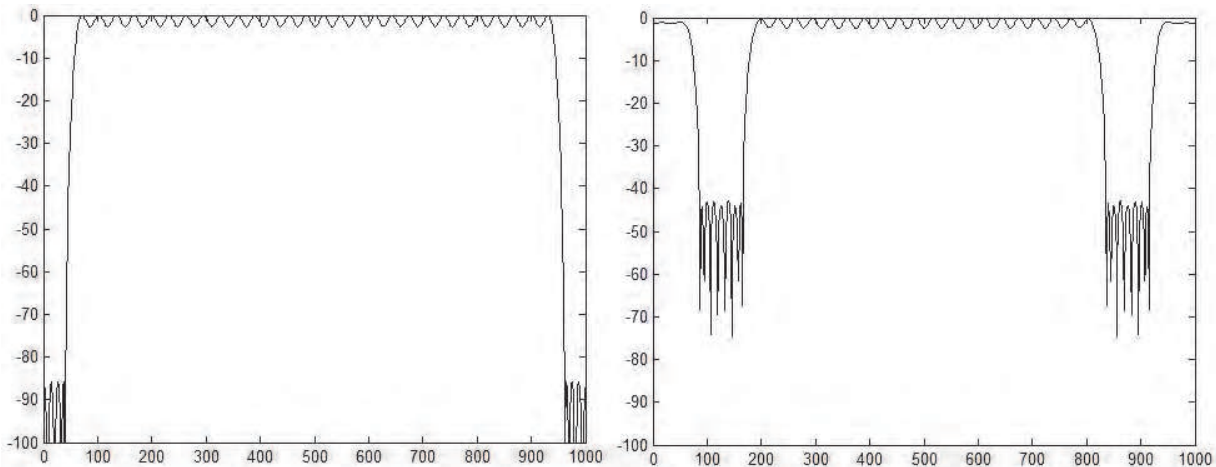


Fig. 12a. Tunable band pass $\omega_0 = 0$ $[H(z)H(z)]$ Fig. 12b. Tunable band pass $\omega_0 = \pi/4$

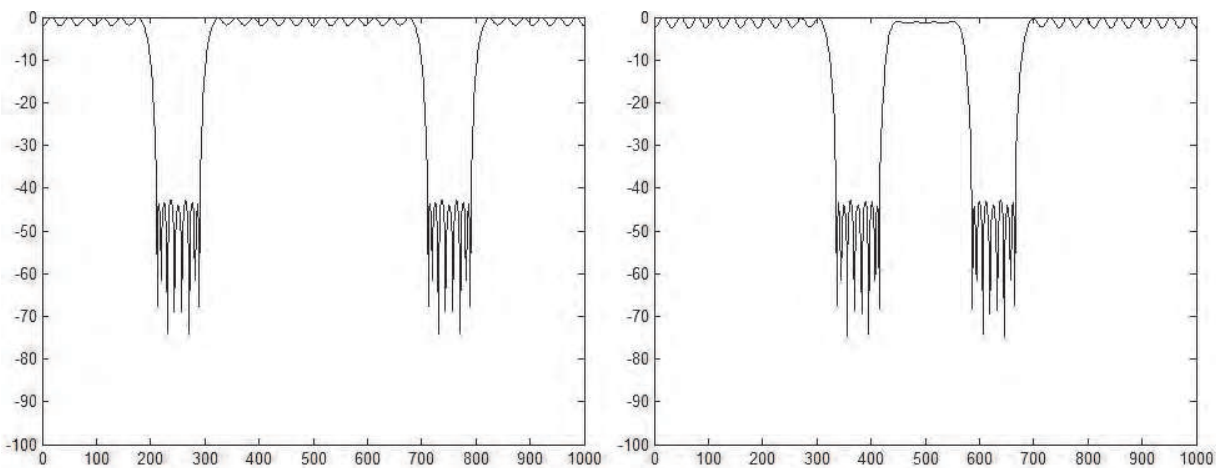


Fig. 12c. Tunable band pass $\omega_0 = \pi/2$ Fig. 12d. Tunable band pass $\omega_0 = 3\pi/4$

Fig. 12. Tunable center-frequency linear-phase band-stop filter using the three-way Complex heterodyne circuit

3.2 Tunable cut-off frequency low-pass filter

To design a tunable cut-off frequency low-pass filter, the prototype filter must be a wide-band low-pass filter with the bandwidth equal to half the Nyquist Frequency. Before calling the MatLab m-file `n3wayhet`, we initialize the input variables as follows:

```
inp=1;npoints=1000;w0=0;a=1;b=firpm(64,[0 .5*.955 .5/.955 1],[1 1 0 0],[1 10]);
scale=1;n3wayhet
```

Figure 13 shows the design criteria for the prototype low-pass filter with cut-off frequency at $\pi/2$ that is needed to implement the tunable cut-off frequency low-pass filter. The prototype low-pass filter needs a cut-off frequency of $\pi/2$. The prototype filter must have one-half the pass-band ripple of the desired pass-band ripple and the same stop band attenuation as for the tunable cut-off frequency low-pass filter.

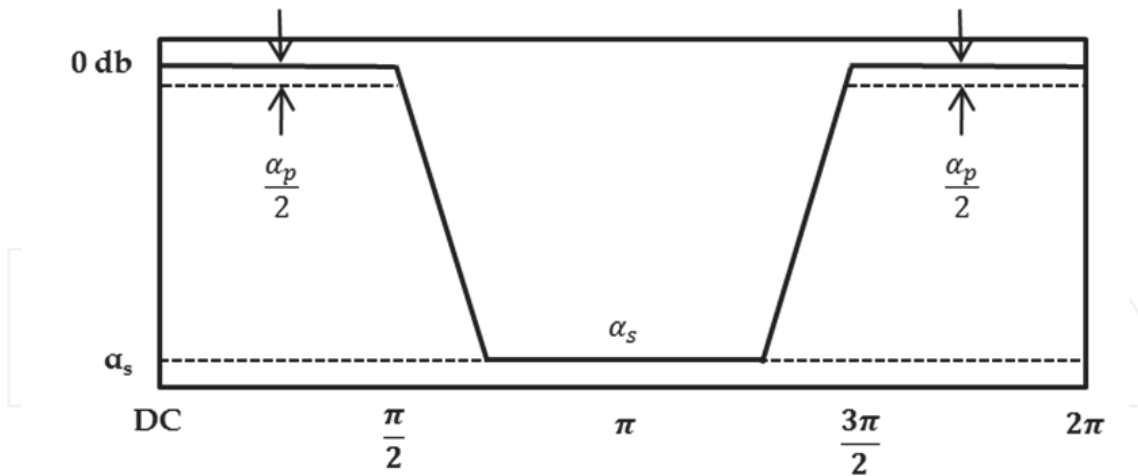


Fig. 13. Design criteria for prototype low-pass filter $H(z)$ with cut-off frequency at $\pi/2$ required to implement a tunable cut-off frequency low-pass filter using the three-way complex heterodyne circuit of Figure 9.

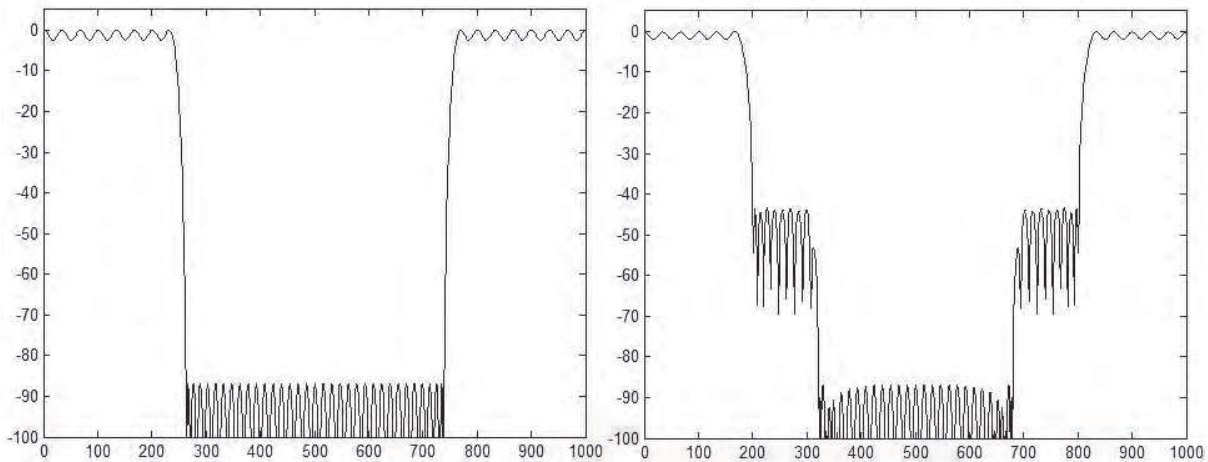


Fig. 14a. Tunable cut-off low-pass $\omega_0 = 0$ [$H(z)H(z)$] Fig. 14b. Tunable cut-off low-pass $\omega_0 = \pi/4$

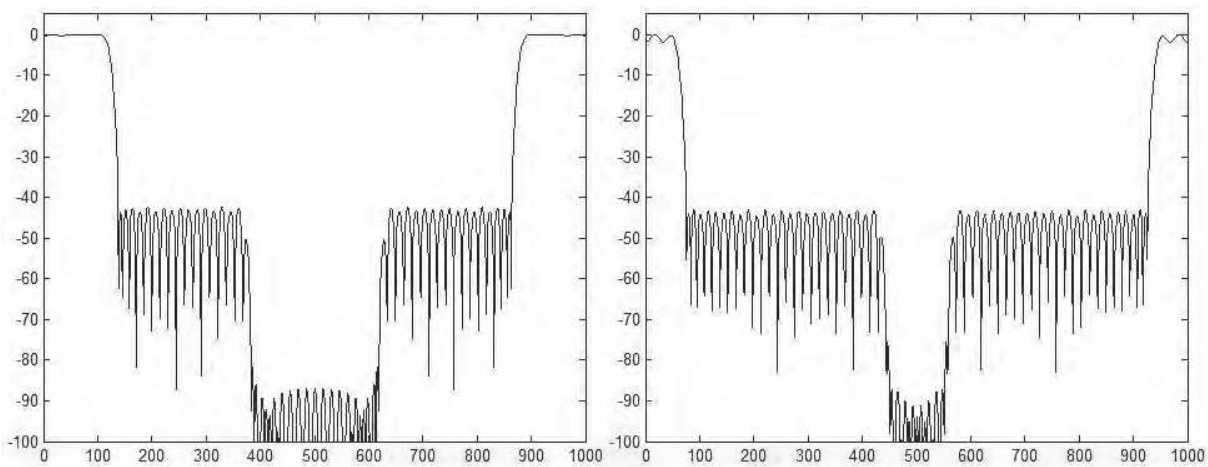


Fig. 14c. Tunable cut-off low-pass $\omega_0 = \pi/2$

Fig. 14d. Tunable cut-off low-pass $\omega_0 = 3\pi/4$

Fig. 14. Tunable cut-off frequency linear-phase low-pass filter using three-way complex heterodyne circuit

Figure 14 shows the tunable cut-off frequency low-pass filter. First, when $\omega_0 = 0$ we get the frequency response shown in Figure 14a which is the prototype filter convolved with itself ($H(z)H(z)$). Thus we have over 80db attenuation in the stop band and the desired less than 3db ripple in the pass-band. The prototype filter is Low-Pass with bandwidth set to one-half the Nyquist frequency (250 on the x-axis). Figure 14b shows the circuit with $\omega_0 = \pi/8$. This tunes the cut-off frequency to $\pi/2 - \pi/8 = 3\pi/8$ which shows up as 187.5 on the x-axis of Figure 14b. Figure 14c shows the circuit with $\omega_0 = \pi/4$. This tunes the cut-off frequency to $\pi/2 - \pi/4 = \pi/4$ which shows up as 125 on the x-axis of Figure 14c. Figure 14d shows the circuit with $\omega_0 = 3\pi/8$. This tunes the center frequency to $\pi/2 - 3\pi/8 = \pi/8$ which shows up as 62.5 on the x-axis of Figure 14d. Notice that the attenuation of the tuned low-pass filters is over 40db which is the same stop-band attenuation as the prototype filter. All of these filters retain the linear-phase property of the prototype filter that was designed using the Parks-McClellan algorithm.

3.3 Tunable cut-off frequency high-pass filter

To design a tunable cut-off frequency high-pass filter, the prototype filter must be a wide-band high-pass filter with the bandwidth equal to half the Nyquist Frequency. Before calling the MatLab m-file `n3wayhet`, we initialize the input variables as follows:

```
inp=1;npoints=1000;w0=0;a=1;b=firpm(64,[0 .1*.8 .1/.8 1],[0 0 1 1],[10 1]);
scale=1;n3wayhet;
```

Figure 15 shows the design criteria for the prototype high-pass filter with cut-off frequency at $\pi/2$ that is needed to implement the tunable cut-off frequency high-pass filter. The prototype high-pass filter needs a cut-off frequency of $\pi/2$. The prototype filter must have one-half the pass-band ripple of the desired pass-band ripple and the same stop band attenuation as for the tunable cut-off frequency high-pass filter.

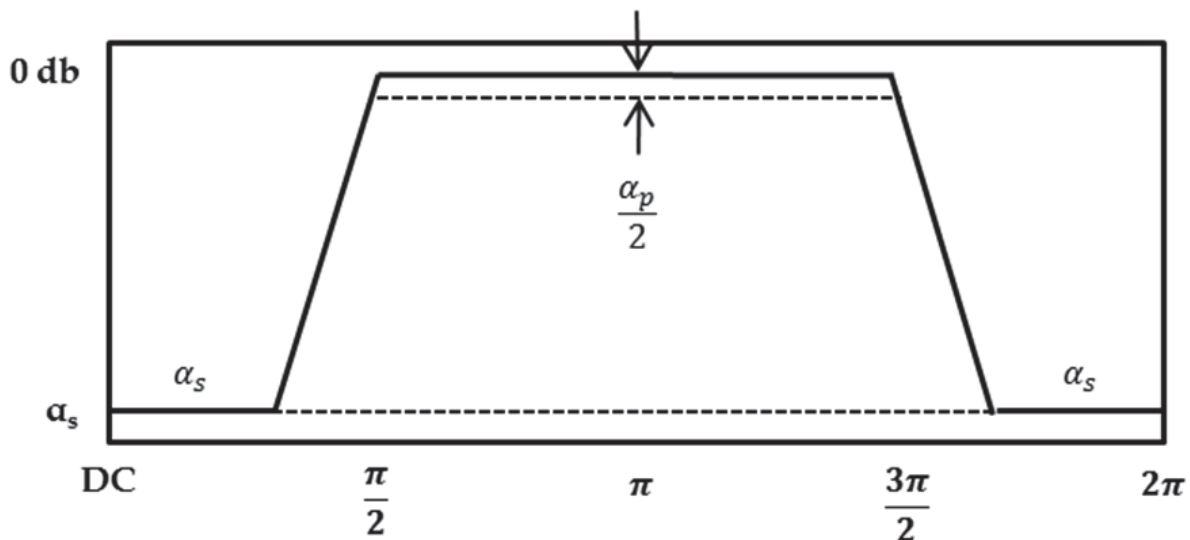


Fig. 15. Design criteria for prototype high-pass filter $h(z)$ with cut-off frequency at $\pi/2$ required to implement a tunable cut-off frequency high-pass filter using the three-way complex heterodyne circuit of figure 9.

Figure 16 shows the tunable cut-off frequency high-pass filter. First, when $\omega_0 = 0$ we get the frequency response shown in Figure 16a which is the prototype filter convolved with itself ($H(z)H(z)$). Thus we have over 80db attenuation in the stop band and the desired less than 3db ripple in the pass-band. The prototype filter is High-Pass with bandwidth set to one-half the Nyquist frequency (250 on the x-axis). Figure 16b shows the circuit with $\omega_0 = \pi/8$. This tunes the cut-off frequency to $\pi/2 + \pi/8 = 5\pi/8$ which shows up as 312.5 on the x-axis of Figure 16b. Figure 16c shows the circuit with $\omega_0 = \pi/4$. This tunes the cut-off frequency to $\pi/2 + \pi/4 = 3\pi/4$ which shows up as 375 on the x-axis of Figure 16c. Figure 16d shows the circuit with $\omega_0 = 3\pi/8$. This tunes the center frequency to $\pi/2 + 3\pi/8 = 7\pi/8$ which shows up as 437.5 on the x-axis of Figure 16d. Notice that the attenuation of the tuned high-pass filters is over 40db which is the same stop-band attenuation as the prototype filter. All of these filters retain the linear-phase property of the prototype filter that was designed using the Parks-McClellan algorithm.

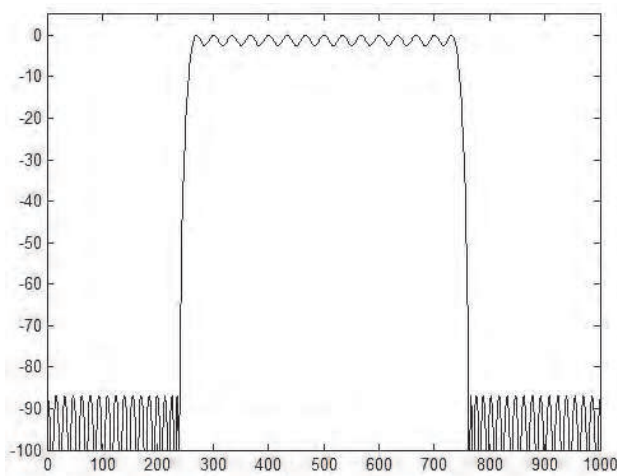
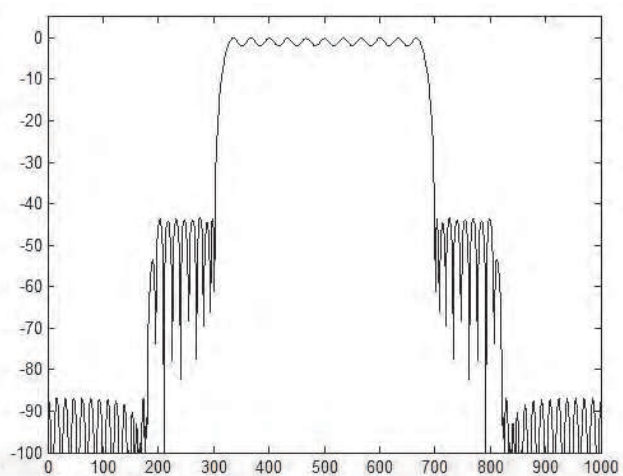
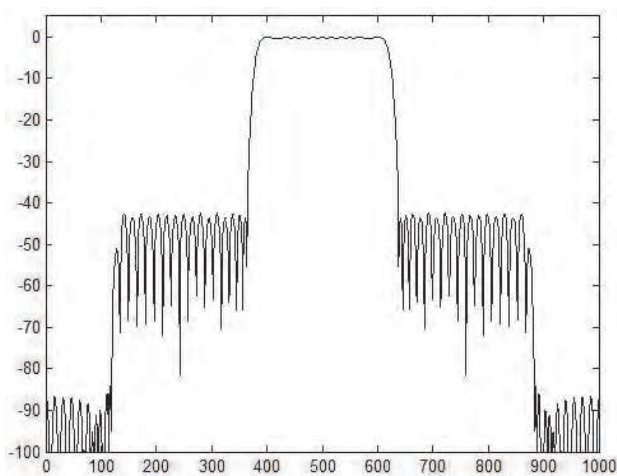
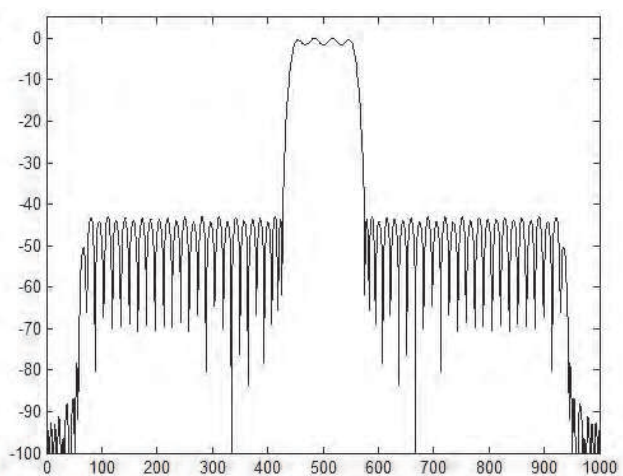
Fig. 16a. Tunable high-pass filter $\omega_0 = 0$ ($H(z)H(z)$)Fig. 16b. Tunable high-pass filter $\omega_0 = \pi/8$ Fig. 16c. Tunable high-pass filter $\omega_0 = \pi/4$ Fig. 16d. Tunable high-pass filter $\omega_0 = 3\pi/8$

Fig. 16. Tunable cut-off frequency linear-phase high-pass filter using three-way complex heterodyne circuit

3.4 Tunable bandwidth band-pass filter

To design a tunable bandwidth band-pass filter, the prototype filter must be a wide-band band-pass filter with the bandwidth equal to half the Nyquist Frequency. Before calling the MatLab m-file `n3wayhet`, we initialize the input variables as follows:

```
inp=1;npoints=1000;w0=0;a=1;b=firpm(64,[0 .25*.9 .25/.9 .75*.95 .75/.95 1],
    [0 0 1 1 0 0],[10 1 10]);scale=1;n3wayhet
```

Figure 17 shows the design criteria for the prototype band-pass filter with bandwidth of $\pi/2$ that is needed to implement the tunable bandwidth band-pass filter. The prototype band-pass filter needs a bandwidth of $\pi/2$. The prototype filter must have one-half the pass-band ripple of the desired pass-band ripple and the same stop band attenuation as for the tunable bandwidth band-pass filter.

Figure 18 shows the tunable bandwidth band-pass filter. First, when $\omega_0 = 0$ we get the frequency response shown in Figure 18a which is the prototype filter convolved with itself ($H(z)H(z)$). Thus we have over 80db attenuation in the stop band and the desired less than 3db ripple in the pass-band. The prototype filter is Band-Pass centered at $\pi/2$ with bandwidth of $\pi/2$ (125 to 375 on the x-axis). Figure 18b shows the circuit with $\omega_0 = \pi/16$. This tunes the lower band edge to $\pi/2 - \pi/4 + \pi/16 = 5\pi/16$ (156.25 on the x-axis of Figure 18b) and the upper band edge to $\pi/2 + \pi/4 - \pi/16 = 11\pi/16$ (343.75 on the x-axis of Figure 18b). Figure 18c shows the circuit with $\omega_0 = \pi/8$. This tunes the lower band edge to $\pi/2 - \pi/4 + \pi/8 = 3\pi/8$ (187.5 on the x-axis of Figure 16c) and the upper band edge to $\pi/2 + \pi/4 - \pi/8 = 5\pi/8$ (312.5 on the x-axis in Figure 18c). Figure 18d shows the circuit with $\omega_0 = 3\pi/16$. This tunes the lower band edge to $\pi/2 - \pi/4 + 3\pi/16 = 7\pi/16$ (218.75 on the x-axis of Figure 18d) and the upper band edge to $\pi/2 + \pi/4 - 3\pi/16 = 9\pi/16$ (281.25 on the x-axis of Figure 18d). Notice that the attenuation of the tuned band-pass filters is over 40db which is the same stop-band attenuation as the prototype filter. All of these filters retain the linear-phase property of the prototype filter that was designed using the Parks-McClellan algorithm.

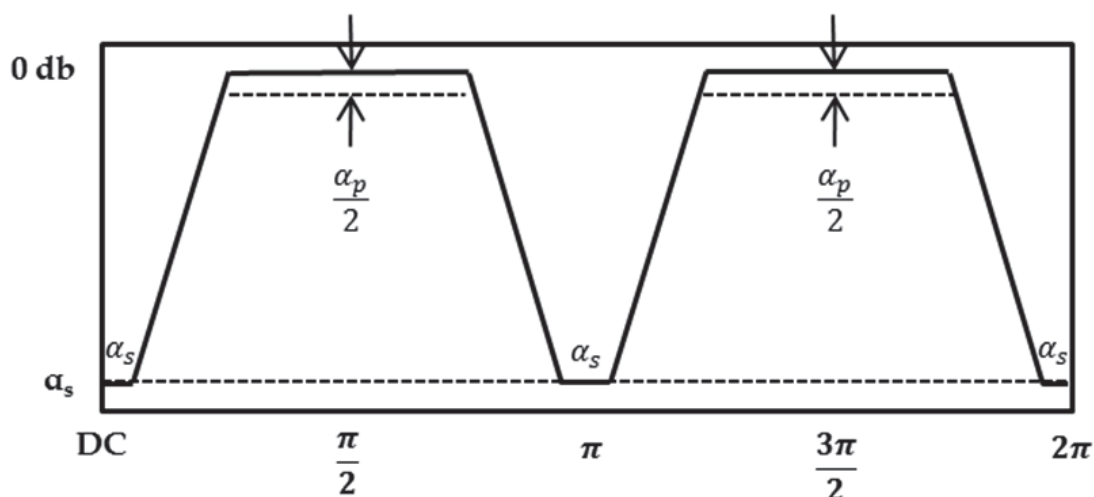


Fig. 17. Design criteria for prototype band-pass filter $h(z)$ centered at $\pi/2$ with bandwidth of $\pi/2$ (band edges at $\pi/4$ and $3\pi/4$) required to implement a tunable bandwidth band-pass filter using the three-way complex heterodyne circuit of figure 9.

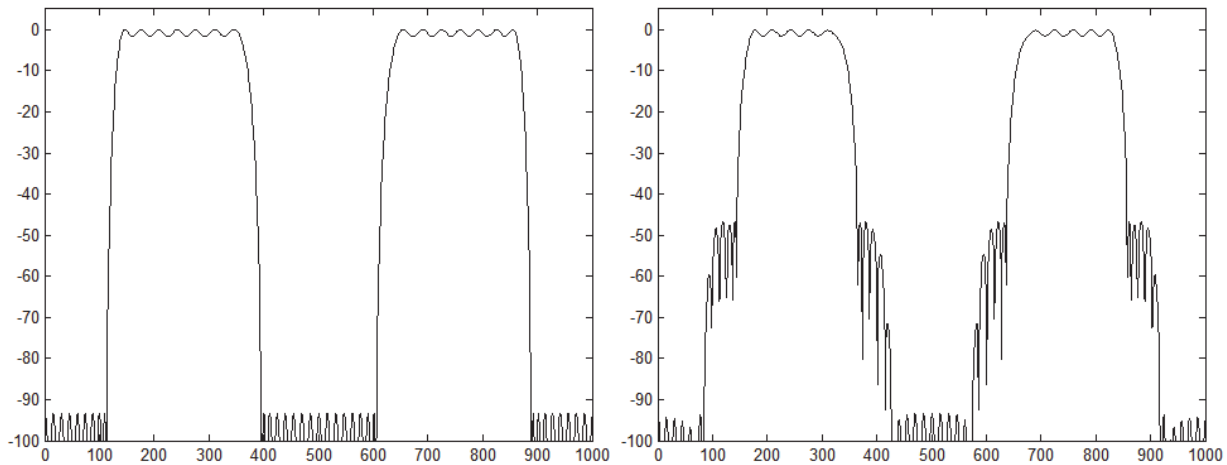


Fig. 18a. Tunable bandwidth BP filter $\omega_0 = 0$ ($H(z)H(z)$) Fig. 18b. Tunable bandwidth BP filter $\omega_0 = \pi/8$

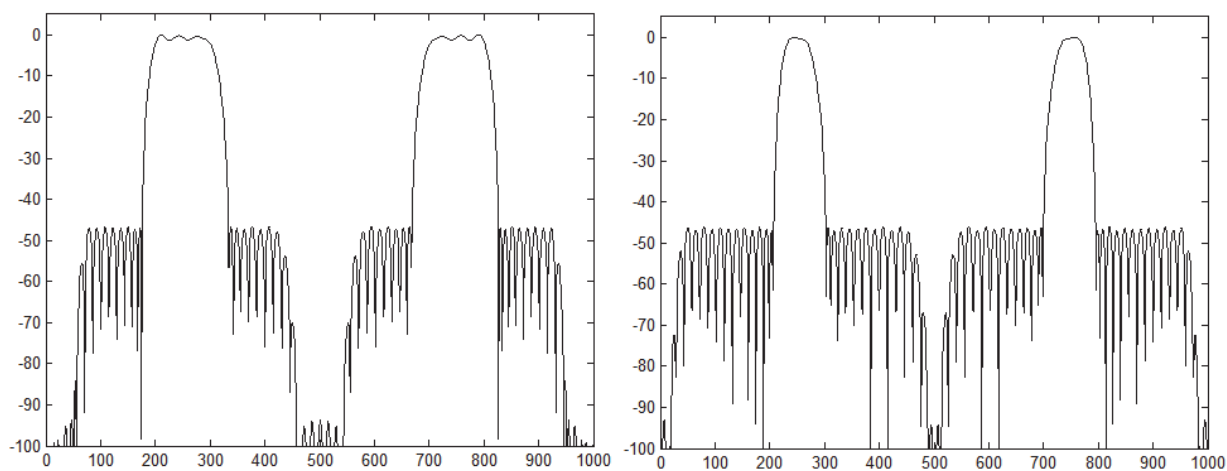


Fig. 18c. Tunable bandwidth BP filter $\omega_0 = \pi/4$ Fig. 18d. Tunable bandwidth BP filter $\omega_0 = 3\pi/8$

Fig. 18. Tunable bandwidth linear-phase band-pass filter using three-way complex heterodyne circuit

3.5 Tunable bandwidth band-stop filter

To design a tunable bandwidth band-stop filter, the prototype filter must be a wide-band band-stop filter with the bandwidth equal to half the Nyquist Frequency. Before calling the MatLab m-file `n3wayhet`, we initialize the input variables as follows:

```
inp=1;npoints=1000;w0=0;a=1;b=firpm(64,[0 .25*.9 .25/.9 .75*.95 .75/.95 1],[1 1 0 0 1 1],
[1 10 1]);scale=1;n3wayhet
```

Figure 19 shows the design criteria for the prototype band-stop filter with bandwidth of $\pi/2$ that is needed to implement the tunable bandwidth band-stop filter. The prototype band-stop filter needs a bandwidth of $\pi/2$. The prototype filter must have one-half the pass-band ripple of the desired pass-band ripple and the same stop band attenuation as for the tunable bandwidth band-stop filter.

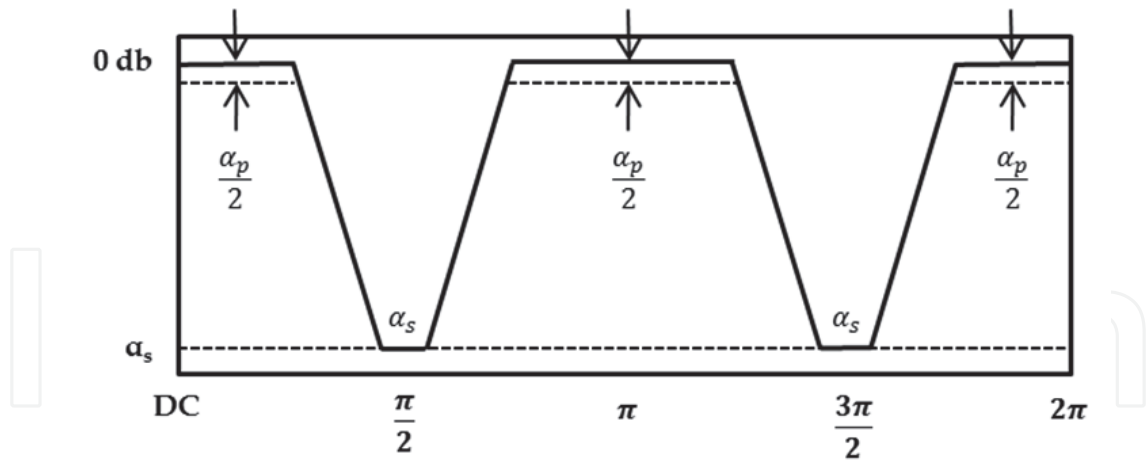


Fig. 19. Design criteria for prototype band-stop filter $H(z)$ centered at $\pi/2$ with bandwidth of $\pi/2$ (band edges at $\pi/4$ and $3\pi/4$) required to implement a tunable bandwidth band-stop filter using the three-way complex heterodyne circuit of Figure 9.

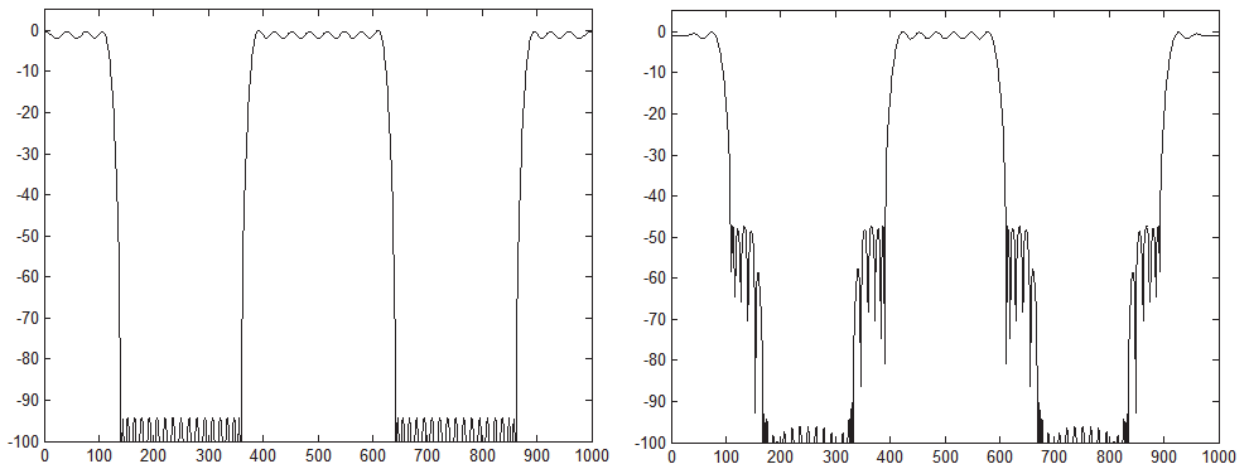


Fig. 20a. Tunable bandwidth BS filter $\omega_0 = 0$ ($H(z)H(z)$) Fig. 20b. Tunable bandwidth BS filter $\omega_0 = \pi/8$

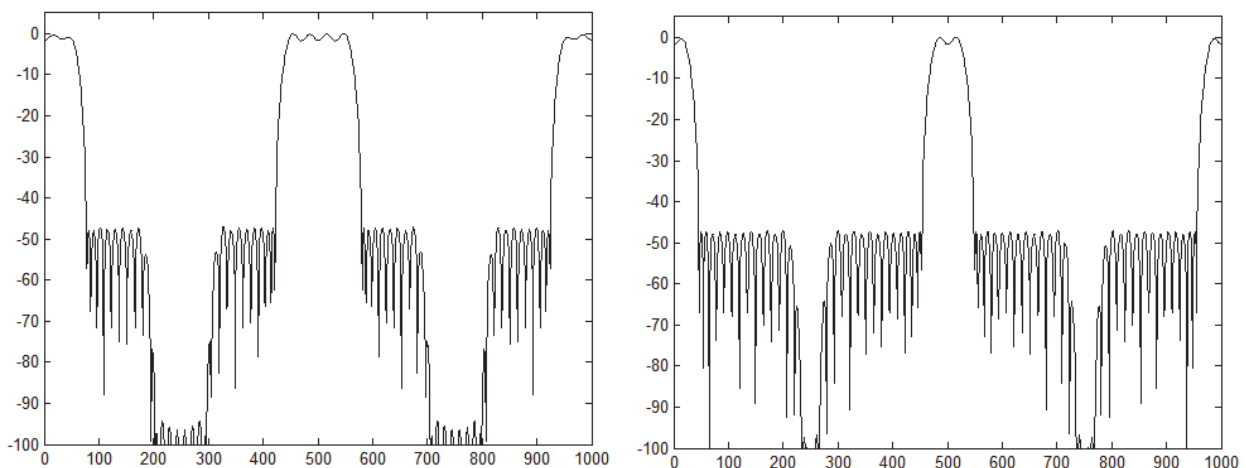


Fig. 20c. Tunable bandwidth BS filter $\omega_0 = \pi/4$ Fig. 20d. Tunable bandwidth BS filter $\omega_0 = 3\pi/8$

Fig. 20. Tunable bandwidth linear-phase band-stop filter using three-way complex heterodyne circuit

Figure 20 shows the tunable bandwidth band-stop filter. First, when $\omega_0 = 0$ we get the frequency response shown in Figure 20a which is the prototype filter convolved with itself ($H(z)H(z)$). Thus we have over 80db attenuation in the stop band and the desired less than 3db ripple in the pass-band. The prototype filter is Band-Stop centered at $\pi/2$ with bandwidth of $\pi/2$ (125 to 375 on the x-axis). Figure 20b shows the circuit with $\omega_0 = \pi/16$. This tunes the lower band edge to $\pi/2 - \pi/4 + \pi/16 = 5\pi/16$ (156.25 on the x-axis of Figure 18b) and the upper band edge to $\pi/2 + \pi/4 - \pi/16 = 11\pi/16$ (343.75 on the x-axis of Figure 20b). Figure 20c shows the circuit with $\omega_0 = \pi/8$. This tunes the lower band edge to $\pi/2 - \pi/4 + \pi/8 = 3\pi/8$ (187.5 on the x-axis of Figure 20c) and the upper band edge to $\pi/2 + \pi/4 - \pi/8 = 5\pi/8$ (312.5 on the x-axis in Figure 20c). Figure 20d shows the circuit with $\omega_0 = 3\pi/16$. This tunes the lower band edge to $\pi/2 - \pi/4 + 3\pi/16 = 7\pi/16$ (218.75 on the x-axis of Figure 20d) and the upper band edge to $\pi/2 + \pi/4 - 3\pi/16 = 9\pi/16$ (281.25 on the x-axis of Figure 20d). Notice that the attenuation of the tuned band-stop filters is over 40db which is the same stop-band attenuation as the prototype filter. All of these filters retain the linear-phase property of the prototype filter that was designed using the Parks-McClellan algorithm.

3.6 Summary of three-way tunable complex heterodyne filter (Azam's technique)

The Three-Way Complex Heterodyne Technique is capable of designing tunable center frequency band-stop and notch filter, tunable cut-off frequency low-pass and high-pass filters and tunable bandwidth band-pass and band-stop filters. The technique is not able to implement tunable center-frequency band-pass filters, but these are easily implementable by the simple cosine heterodyne circuit of Figure 2.

Figure 9 is the basic Three-Way Complex Heterodyne Circuit used to implement these filters in software or hardware. A very nice FPGA implementation of this circuit has been reported in the literature in a paper that won the Myril B. Reed Best Paper Award at the 2000 IEEE International Midwest Symposium on Circuits and Systems (Azam et. al., 2000). For further information on this paper and the award, visit the MWSCAS web page at <http://mwscas.org>. Table 1 provides the design details for the five possible tunable filters. Sections 3.1 through 3.5 provide examples of each of the five tunable filters from Table 1. In section 6 of this chapter we shall show how to make these tunable filters adaptive so that they can automatically vary center frequency, cut-off frequency or bandwidth to adapt to various signal processing needs.

4. Bottom-top tunable complex heterodyne filters (Cho's technique)

The Three-Way Tunable Complex Heterodyne Circuit of section 3 implemented by the circuit of Figure 9 is a special case of a more general technique referred to as the Bottom-Top Tunable Complex Heterodyne Filter Technique. Figure 21 below shows the complete circuit for the Bottom-Top Tunable Complex Heterodyne Filter:

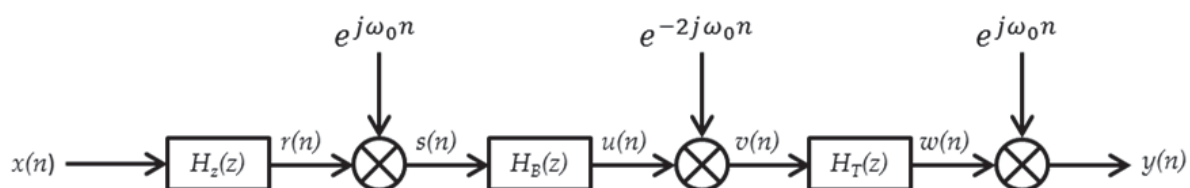


Fig. 21. Bottom-top tunable complex heterodyne circuit (Cho's technique)

Comparing the circuit of Figure 21 to the circuit of Figure 9, we see that the circuit of Figure 21 has one additional fixed filter block $H_z(z)$ between the input and the first heterodyne stage. This block allows for fixed signal processing that is not subject to the rotations of the other two blocks. Otherwise, this is the same circuit as Figure 9. However, the addition of this extra block gives us the flexibility to do many more signal processing operations.

We do not have sufficient room in this chapter to explore all the possibilities of the circuit of Figure 9, so we shall limit ourselves to three: (1) Tunable filters with at least some real poles and zeros, (2) Tunable filters with poles and zeros clustered together on the unit circle, and (3) Tunable filters realized with a Nyquist filter that allows the elimination of the last heterodyne stage. This third option is so important that we will cover it as a separate topic in section 5. The first two are covered here in section 4.1 and 4.2 respectively.

4.1 Tunable filters with real poles and zeros

When the prototype filter has some of its poles and zeros located on the real axis, it is often useful to remove these poles and zeros from the rotation process and allow them to remain on the real axis. An example of this is the design of a tunable cut-off frequency low-pass (or high-pass) filter. Such filters typically have some poles and zeros on the real axis. An excellent example of this is a Butterworth Low-Pass Filter. An n^{th} order Butterworth Filter has n zeros located at -1 on the real axis. If we wish to design a tunable cut-off frequency Butterworth Low-Pass Filter, the prototype filter will have a cut-off frequency at $\pi/2$. The only other specification for a Butterworth Filter is the order of the filter. Here we pick an 11th order Butterworth Low-Pass Filter with cut-off frequency of $\pi/2$:

```
[b,a]=butter(11,0.5);
```

To design a tunable cut-off frequency low-pass filter using the circuit of Figure 21, we will divide the poles and zeros of the prototype filter between the three transfer function boxes such that $H_z(z)$ contains all the real poles and zeros, $H_B(z)$ contains all the complex poles and zeros with negative imaginary parts (those located in the bottom of the z -plane) and $H_T(z)$ contains all the complex poles and zeros with positive imaginary parts (those located in the top of the z -plane). The following MatLab m-file accomplishes this:

```
% BOTTOMTOP
% Extracts the bottom and top poles and zeros from a filter
function
% INPUT: [b,a] = filter coefficients
%        delta = maximum size of imaginary part to consider
it zero
% OUTPUT:
%        [bz,az] = real poles and zeros
%        [bb,ab] = bottom poles and zeros
%        [bt,at] = top poles and zeros
clear rb rbz rbt rbb ra raz rat rab bz bt bb az at ab
rb=roots(b);
lb=length(b)-1;
% find real zeros
rbz=1;
nbz=0;
nbt=0;
nbb=0;
for index=1:lb
```

```

        if abs(imag(rb(index))) < delta
            nbz = nbz + 1;
            rbz(nbz, 1) = real(rb(index));
% find top zero
            elseif imag(rb(index)) > 0
                nbt = nbt + 1;
                rbt(nbt, 1) = rb(index);
% find bottom zero
            else
                nbb = nbb + 1;
                rbb(nbb, 1) = rb(index);
            end
        end
    end
    ra = roots(a);
    la = length(a) - 1;
% find real poles
    raz = 1;
    naz = 0;
    nat = 0;
    nab = 0;
    for index = 1:la
        if abs(imag(ra(index))) < delta
            naz = naz + 1;
            raz(naz, 1) = real(ra(index));
% find top zero
            elseif imag(ra(index)) > 0
                nat = nat + 1;
                rat(nat, 1) = ra(index);
% find bottom zero
            else
                nab = nab + 1;
                rab(nab, 1) = ra(index);
            end
        end
    end
    if nbz == 0
        bz = 1;
    else
        bz = poly(rbz);
    end
    if nbt == 0
        bt = 1;
    else
        bt = poly(rbt);
    end
    if nbb == 0
        bb = 1;
    else
        bb = poly(rbb);
    end
    if naz == 0
        az = 1;
    else
        az = poly(raz);
    end

```

```

end
if nat==0
    at=1;
else
    at=poly(rat);
end
if nab==0
    ab=1;
else
    ab=poly(rab);
end

```

Figure 22 shows the results of applying the above m-file to the prototype 11th order Butterworth Low-Pass Filter with cut-off frequency at $\pi/2$.

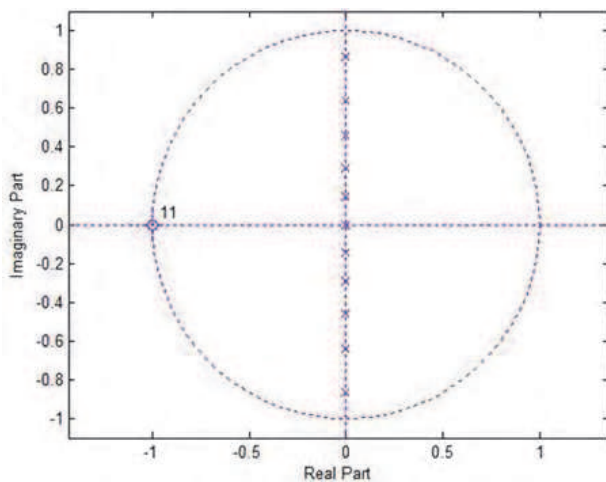


Fig. 22a. Pole-zero plot of $H(z)$
(11th order butterworth LP)

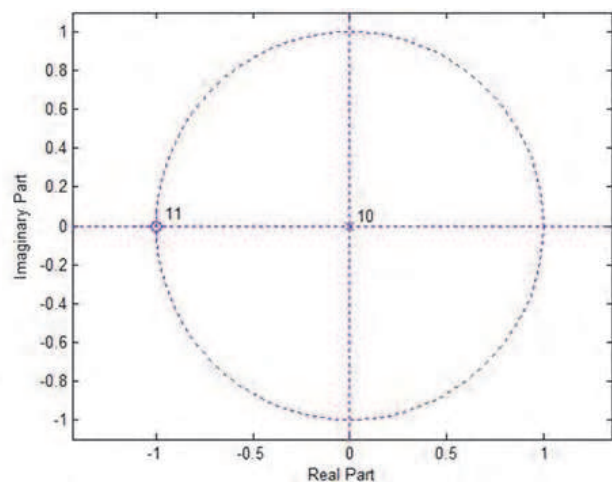


Fig. 22b. Pole-zero plot of $H_z(z)$
(real poles and zeros)

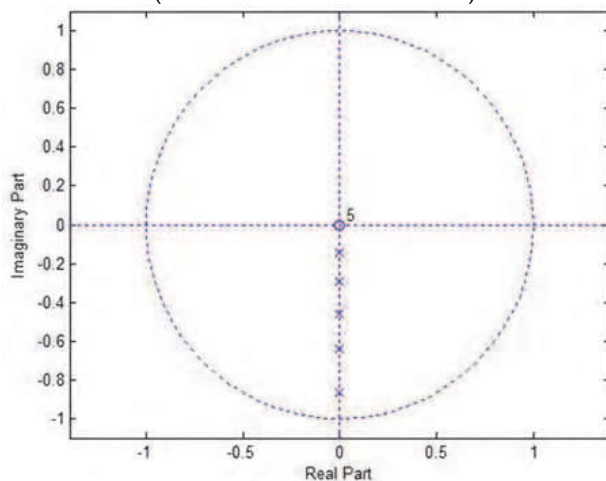


Fig. 22c. Pole-Zero Plot of $H_B(z)$
(bottom poles and zeros).

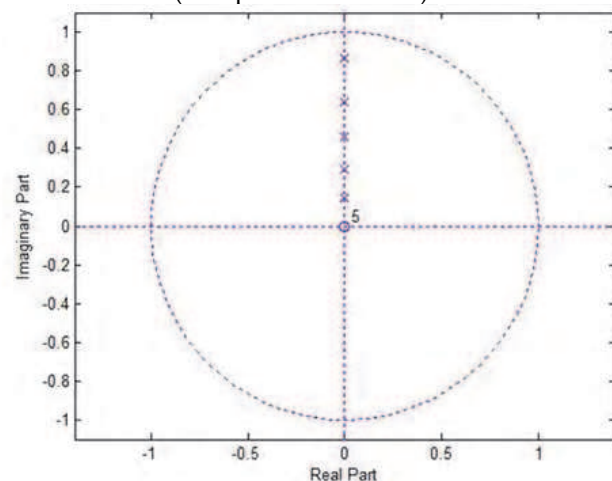


Fig. 22b. Pole-Zero Plot of $H_T(z)$
(top poles and zeros)

Fig. 22. Illustration of the result of the Matlab m-file dividing the poles and zeros in the prototype 11th order butterworth low-pass filter designed with a cut-off frequency of $\pi/2$. The resulting transfer functions $H_z(z)$, $H_B(z)$ and $H_T(z)$ are then implanted in the appropriate boxes in the circuit of Figure 21.

To simulate the Bottom-Top Tunable Complex Heterodyne Filter of Figure 21, we make use of the following MatLab m-file:

```

% CMPLXHET
% Implements the Complex Heterodyne Filter
% INPUTS:
% Set the following inputs before calling 3WAYHET:
%   inp = 0 (provide input file inpf)
%       = 1 (impulse response)
%   npoints = number of points in input
%   w0 = heterodyne frequency
%   [bz az] = coefficients of filter Hz(z)
%   [bb ab] = coefficients of filter Hb(z)
%   [bt at] = coefficients of filter Ht(z)
%   scale = 0 (do not scale the output)
%          = 1 (scale the output to zero db)
%
% OUTPUTS:  ydb = frequency response of the filter
%           hdb, sdb, udb, vdb, wdb (intermediate outputs)
clear y ydb hdb s sdb u udb v vdb w wdb h f
if inp==1
    for index=1:npoints
        inpf(index)=0;
    end
    inpf(1)=1;
end
r=filter(bz,az,inpf);
for index=1:npoints
    s(index)=r(index)*exp(1i*w0*(index-1));
end
u=filter(bb,ab,s);
for index=1:npoints
    v(index)=u(index)*exp(-2*1i*w0*(index-1));
end
w=filter(bt,at,v);
for index=1:npoints
    y(index)=w(index)*exp(1i*w0*(index-1));
end
[h,f]=freqz(b,a,npoints,'whole');
hdb=20*log10(abs(h));
rdb=20*log10(abs(fft(r)));
sdb=20*log10(abs(fft(s)));
udb=20*log10(abs(fft(u)));
vdb=20*log10(abs(fft(v)));
wdb=20*log10(abs(fft(w)));
ydb=20*log10(abs(fft(y)));
if scale==1
    ydbmax=max(ydb)
    ydb=ydb-ydbmax;
end
plot(ydb,'k')

```

Figure 23 shows the results of this simulation for the 11th order Butterworth Low Pass prototype filter with cut-off frequency of $\pi/2$ (250). Figure 23a shows the result for $\omega_0 = 0$. This is the prototype filter. Unlike the Three-Way Tunable Complex Heterodyne Technique of the previous section, we do not need to design for half the desired pass-band ripple. We can design for exactly the desired properties of the tunable filter. Figure 23b shows the result for $\omega_0 = -\pi/8$. This subtracts $\pi/8$ from the cut-off frequency of $\pi/2$ moving the cut-off frequency to $3\pi/8$ (187.5). Figure 23c shows the result for $\omega_0 = -\pi/4$. This subtracts $\pi/4$ from the cut-off frequency of $\pi/2$ moving the cut-off frequency to $\pi/4$ (125). Figure 23d shows the result for $\omega_0 = -3\pi/8$. This subtracts $3\pi/8$ from the cut-off frequency of $\pi/2$ moving the cut-off frequency to $\pi/8$ (62.5). The horizontal line on each of the plots indicates the 3db point for the filter. While there is some peaking in the pass-band as the filter is tuned, it is well within the 3db tolerance of the pass-band.

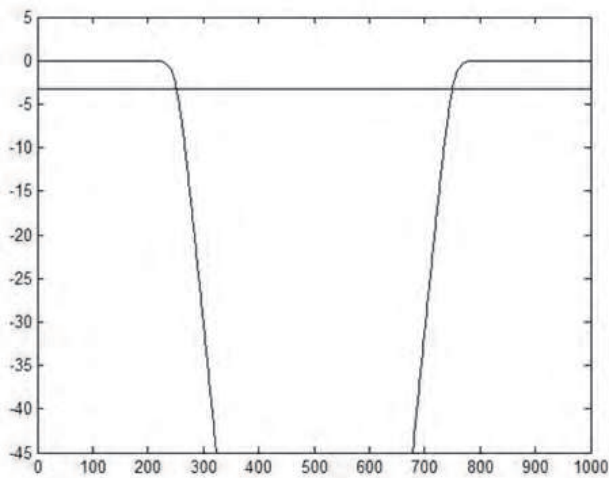


Fig. 23a. Tunable low-pass with $\omega_0 = 0$

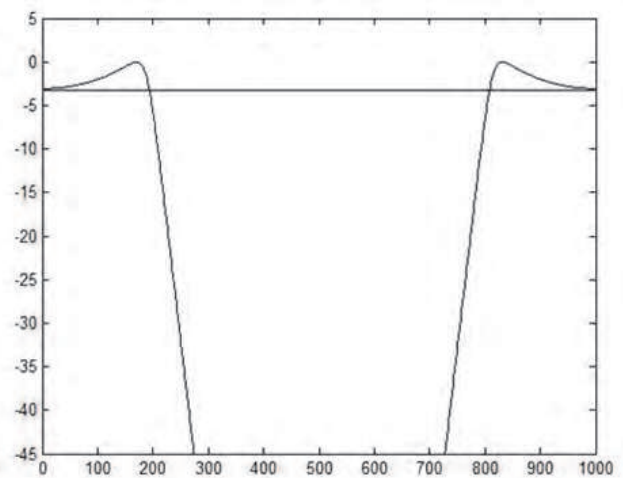


Fig. 23b. Tunable low-pass with $\omega_0 = -\pi/8$

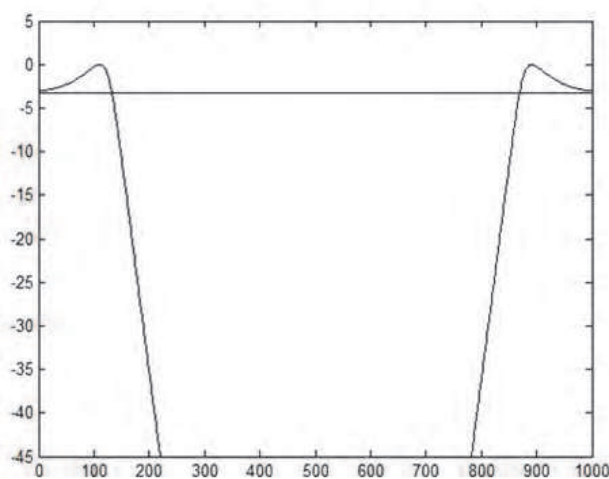


Fig. 23c. Tunable low-pass with $\omega_0 = -\pi/4$

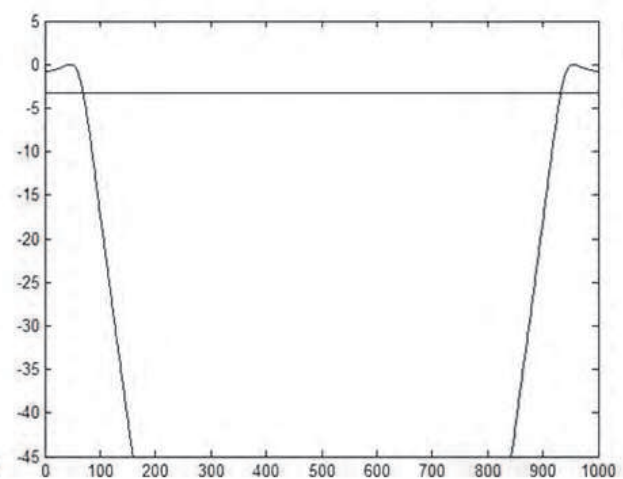


Fig. 23d. Tunable low-pass with $\omega_0 = -3\pi/8$

Fig. 23. Implementation of a tunable cut-off frequency low-pass filter using the bottom-top technique of Figure 21.

4.2 Tunable filters with poles and zeros clustered together on the unit circle

One of the most powerful applications of the Bottom-Top Tunable Complex Heterodyne Technique is its ability to implement the very important tunable center-frequency band-stop filter. Such filters, when made adaptive using the techniques of section 6 of this chapter, are very important in the design of adaptive narrow-band noise attenuation circuits. The Bottom-Top structure of Figure 21 is particularly well suited to the implementation of such filters using any of the designs that result in a cluster of poles and zeros on the unit circle. This is best accomplished by the design of narrow-band notch filters centered at $\pi/2$. All of the IIR design techniques work well for this case including Butterworth, Chebyshev, Inverse Chebyshev and Elliptical Filters.

As an example, we design a Butterworth 5th order band-stop filter and tune it from DC to the Nyquist frequency. In MatLab we use `[b,a]=butter(5,[0.455 0.545], 'stop')`; to obtain the coefficients for the prototype filter. We then use the m-file BOTTOMTOP as before to split the poles and zeros into the proper places in the circuit of Figure 21. Finally, we run the MatLab m-file CMPLXHET to obtain the results shown in Figures 24 and 25.

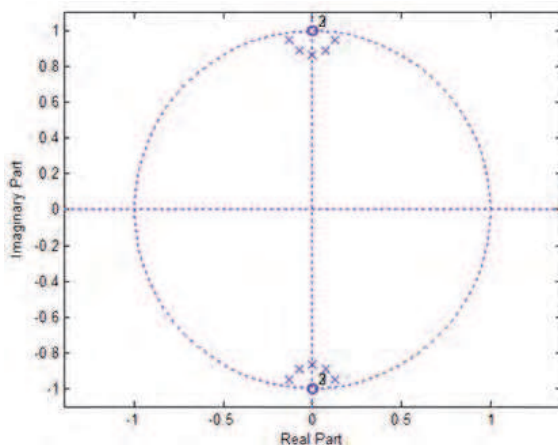


Fig. 24a. Pole-zero plot of prototype band-stop filter

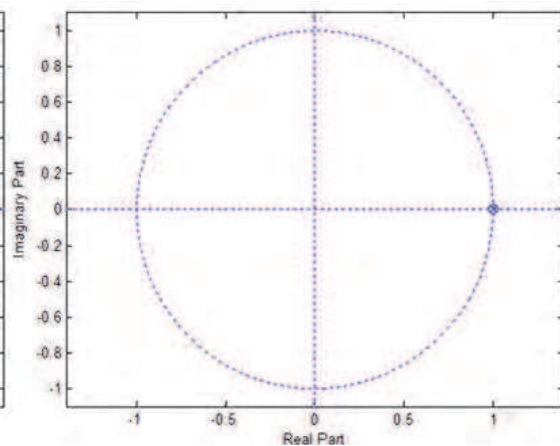


Fig. 24b. Pole zero plot of $H_z(z)$
(real poles and zeros)

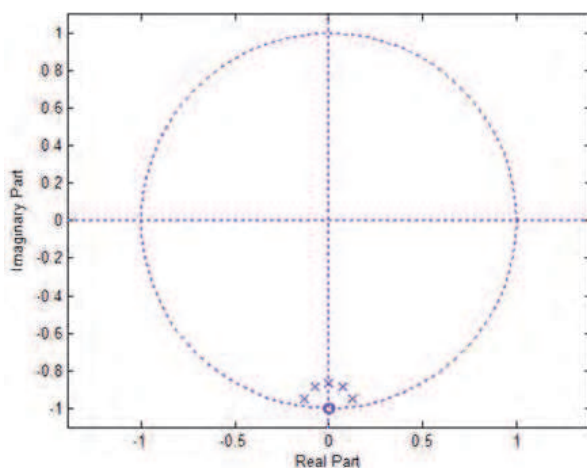


Fig. 24c. Pole-zero plot of $H_b(z)$
(bottom poles & zeros)

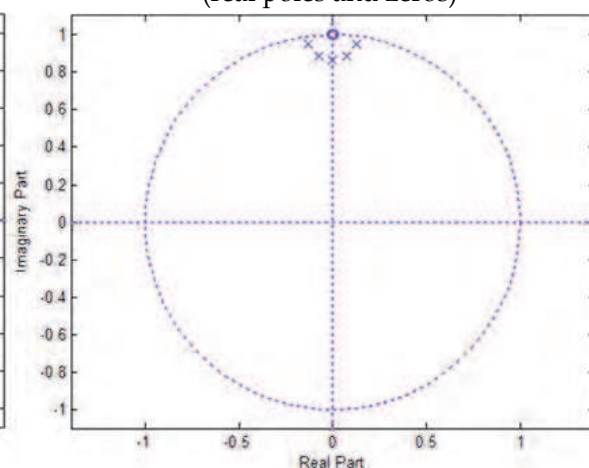


Fig. 24d. Pole zero plot of $H_T(z)$
(top poles & zeros)

Fig. 24. Distribution of poles and zeros for 5th order butterworth band-stop filter centered at $\pi/2$. Notice how the poles and zeros are clustered on the unit circle. This is the ideal case of use of the bottom-top tunable complex heterodyne filter circuit of Figure 21.

Figure 24 shows the poles and zeros clustered in the z -plane on the unit circle. Figure 24a. shows the poles and zeros of the prototype 5th order Butterworth band-stop filter centered at $\pi/2$ designed by `[b,a]=butter(5,[0.455 0.545], 'stop')`. Figure 24b shows the poles and zeros assigned to $H_z(z)$ by the MatLab m-file BOTTOMTOP. Similarly, Figures 24c and 24d show the poles and zeros assigned by the MatLab m-file BOTTOMTOP to $H_B(z)$ and $H_T(z)$ respectively. Figure 25 shows the MatLab simulation of the Bottom-Top Tunable Complex Heterodyne Filter as implemented by the circuit of Figure 21 in the MatLab m-file CMPLXHET. The band-stop center frequency is fully tunable from DC to the Nyquist frequency. The tuned band-stop filter is identical to the prototype band-stop filter. Furthermore, this works for any band-stop design with clustered poles and zeros such as Chebyshev, Inverse Chebyshev and Elliptical designs. In section 6 we shall see how to make these filters adaptive so that they can automatically zero in on narrow-band interference and attenuate that interference very effectively. Figure 25a is for $\omega_0 = 0$, Figure 25b is for $\omega_0 = -7\pi/16$, Figure 25c is for $\omega_0 = -3\pi/16$ and Figure 25d is for $\omega_0 = 5\pi/16$. Note the full tenability form DC to Nyquist.

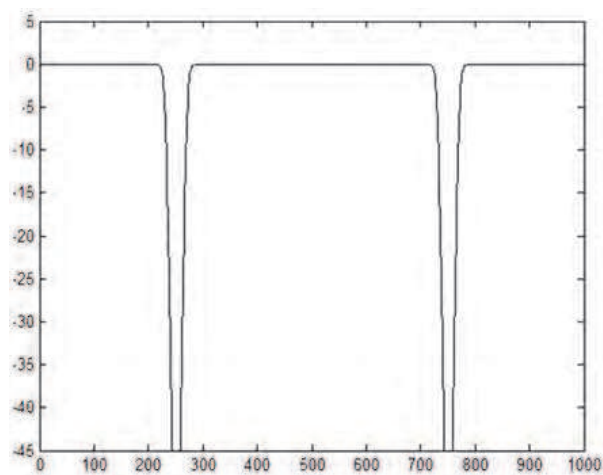


Fig. 25a. Band Stop Tuned to $\pi/2$ ($\omega_0 = 0$)

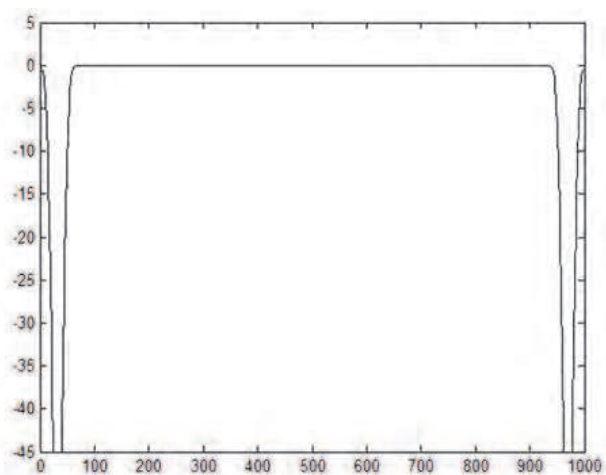


Fig. 25b. Band Stop Tuned to $\pi/16$ ($\omega_0 = -7\pi/16$)

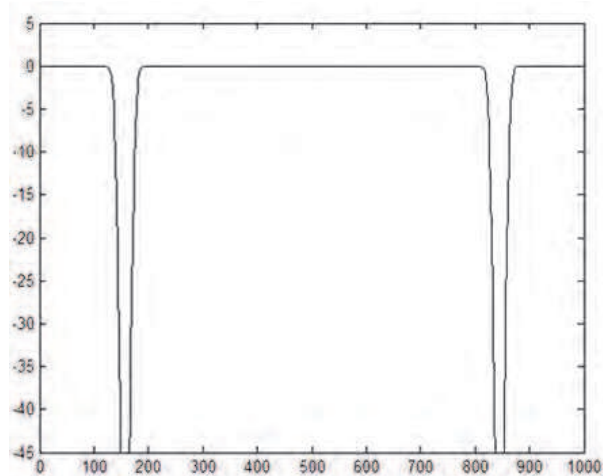


Fig. 25c. Band Stop Tuned to $5\pi/16$ ($\omega_0 = -3\pi/16$)

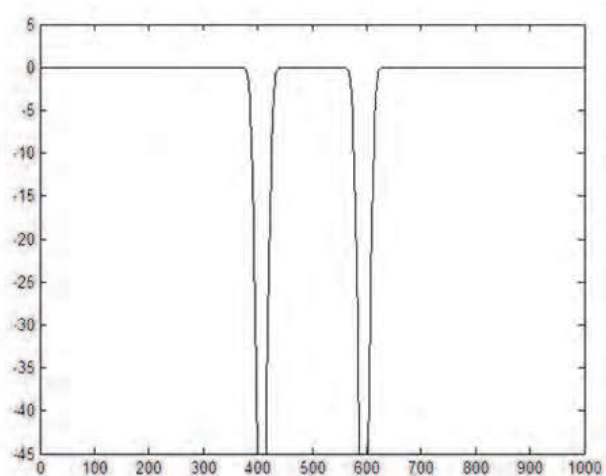


Fig. 25d. Band Stop Tuned to $13\pi/16$ ($\omega_0 = 5\pi/16$)

Fig. 25. Butterworth tunable band-stop filter implemented using bottom-top tunable complex heterodyne technique. Note that the band-stop filter is fully tunable from DC to the Nyquist frequency.

4.3 Summary of bottom-top tunable complex heterodyne filter (Cho's technique)

The Bottom-Top Complex Heterodyne Technique is the most flexible of the heterodyne filter circuits allowing the design of tunable center frequency band-pass, band-stop and notch filter, tunable cut-off frequency low-pass and high-pass filters and tunable bandwidth band-pass and band-stop filters. However, the technique is particularly useful in designing full tunable band-stop filters with characteristics identical to the prototype filter but tunable from DC to the Nyquist frequency.

Figure 21 is the basic Bottom-Top Complex Heterodyne Circuit used to implement these filters in software or hardware. A practical implementation of this circuit has been reported in the literature in a paper appearing in the proceedings of the IEEE International Symposium on Circuit and Systems (Cho, et. al., 2005). The Bottom-Top Complex Heterodyne band-stop filters reported in this paper are aimed at narrow-band attenuation in spread-spectrum radio receivers. In section 6 of this chapter we shall show how to make these tunable filters adaptive so that they can automatically vary center frequency, cut-off frequency or bandwidth to adapt to various signal processing needs.

5. Nyquist tunable complex heterodyne filter technique (Soderstrand's technique)

The final technique for designing Tunable Complex Heterodyne Filters makes use of a modified version of the circuit in Figure 21 shown in Figure 26.

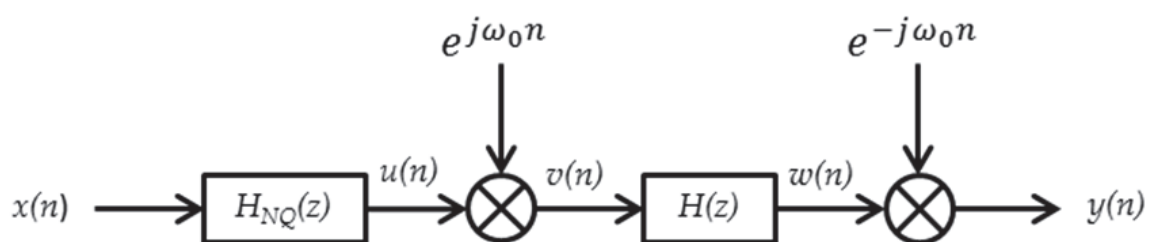


Fig. 26. Nyquist tunable complex heterodyne filter circuit (Soderstrand's technique)

In the circuit of Figure 26 the signal is first passed through $H_{NQ}(z)$, a complex-coefficient digital filter that removes all frequencies from the bottom half of the unit circle in z -plane. Thus this filter removes the negative frequencies or equivalently the frequencies above the Nyquist frequency. Such a filter is easily designed in MatLab by designing a low-pass filter with cut-off frequency of $\pi/2$ and then rotating it in the z -plane so as to pass positive frequencies (frequencies above the real axis in the z -plane) and to attenuate negative frequencies (frequencies below the unit circle in the z -plane).

5.1 Design of the Nyquist Filter $H_{NQ}(z)$

The Nyquist Filter will normally be the same filter regardless of what tunable filter we are realizing. Choice of the Nyquist Filter depends primarily on hardware or software considerations for the target application. If phase is not critical, an IIR Nyquist Filter can be designed using MatLab functions BUTTER, CHEBY, CHEBY2 or ELLIP. However, in many applications phase is of great importance and the Nyquist Filter needs to be designed using the Parks McClellan linear phase technique implemented in MatLab with FIRPM. For our

examples we shall assume that we need a Nyquist Filter with 60db attenuation of the negative frequencies and no more than 1db ripple in the pass-band (positive frequencies). We shall choose a 64-tap filter, although excellent results can be obtained with many fewer taps.

The first step in the design of the Nyquist Filter is to use FIRPM to design a low-pass filter with cut-off frequency at $\pi/2$ with the desired specifications (60db stop-band attenuation and 1db ripple in the pass-band, and 3db attenuation at DC):

```
alp=1;blp=firpm(64,[0 0.45 0.55 1],[1 1 0 0],[1 2]);
```

Figure 27a shows the pole-zero plot of this low-pass filter and Figure 27c shows the frequency response. Note the attenuation at DC is 5db rather than the desired 3db. We shall see this show up in the tunable filter later. In practice we would assure 3db – but we have deliberately left it at 5db to show the effect. We then use MatLab m-file NQFILTER to rotate the low-pass filter by 90 degrees in the z-plane to create the Nyquist Filter whose pole-zero plot is shown in Figure 27b and frequency response in Figure 27d.

```
% NQFILTER
% This script rotates a low-pass filter with a
% cut-off frequency at 0.5 (pi/2) by phi radians
% in the z-plane to create a complex-coefficient
% digital filter that removes the frequencies in
% the lower half of the z-plane (phi = pi/2).
% INPUTS: [blp,alp] = lowpass filter with 0.5 cut-off
%          phi = (suggest pi/2)
% OUTPUTS:
%          [bnq,anq] = the complex-coefficients of
%                    the Nyquist filter
clear nb na bnq anq
nb = length(blp);
na = length(alp);
if nb > 1
    for index=1:nb
        bnq(index)=blp(index)*exp(1i*(index-1)*(phi));
    end
else
    bnq = 1;
end
if na > 1
    for index=1:na
        anq(index)=alp(index)*exp(1i*(index-1)*(phi));
    end
else
    anq = 1;
end
```

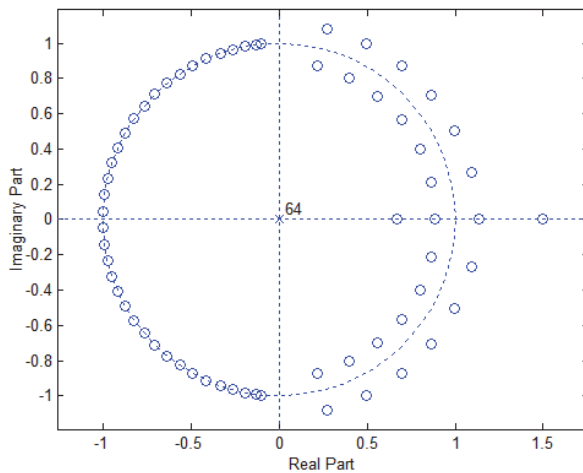


Fig. 27a. Pole-zero plot of low-pass filter

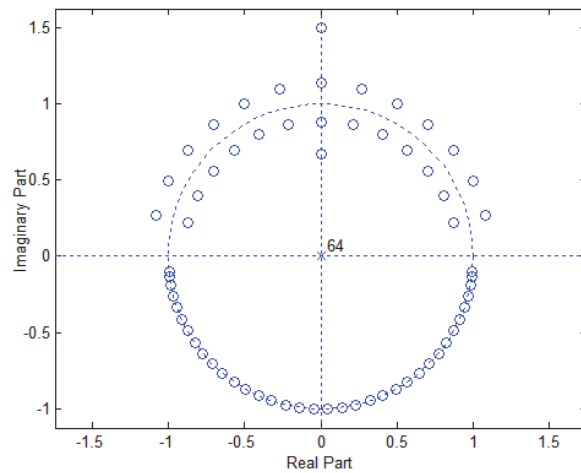


Fig. 27b. Pole-zero plot of nyquist filter

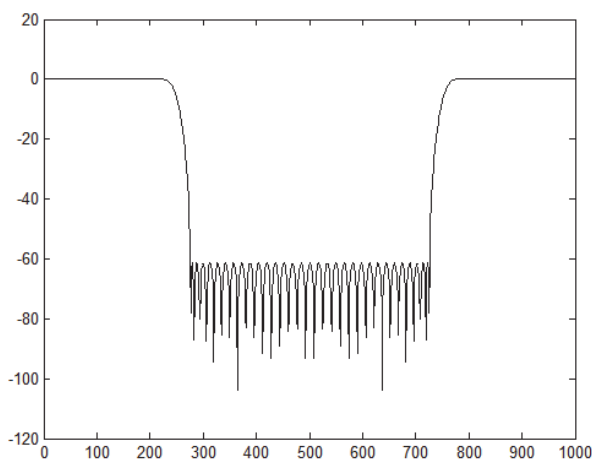


Fig. 27c. Frequency response plot of low-pass filter

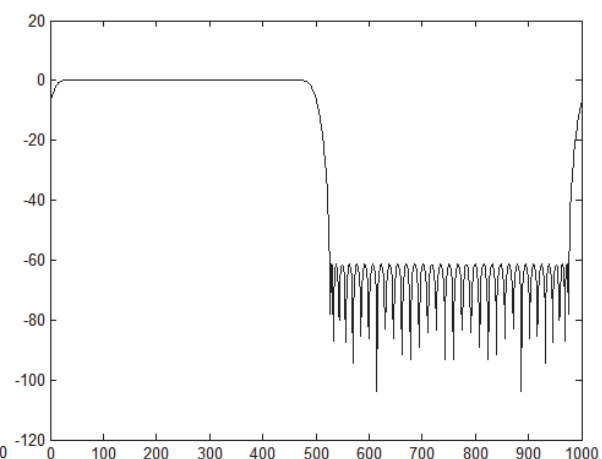


Fig. 27d. Frequency response plot of nyquist filter

Fig. 27. Design of a nyquist filter by rotating a 64-tap parks McClellan linear-phase filter with cut-off frequency at $\pi/2$ by 90 degrees in the z-plane to obtain a filter that attenuates all negative frequencies.

5.2 Novel technique for tuning a complex heterodyne prototype filter (Soderstrand's technique)

Once the negative frequencies have been removed from the input signal, the problem of tuning the filter becomes much simpler. Any prototype filter $H(z)$ may be rotated from its center at DC to its center at ω_0 through the standard rotation technique of Figure 7. This is exactly what is done in the Nyquist Tunable Complex Heterodyne Circuit of Figure 26. The potential problem, however, is that we obtain a filter with all the poles and zeros in the upper half of the z-plane and none in the lower half. Hence the output, $y(n)$, will consist of complex numbers. The novelty of Soderstrand's Technique is that the mirror image poles and zeros needed in the bottom half of the z-plane can be easily created by simply taking the real part of the output $y(n)$. Since we only need the real part of the output, this also simplifies the hardware because we can use the simplified circuit of Figure 6d in the last stage of the circuit of Figure 26. The simulation of the circuit of Figure 26 is accomplished in MatLab with the m-file NQHET:

```

% NQHET (Lab book p. 129 12/11/2010)
% Function to implement Cho complex heterodyne filter
% Set the following inputs before calling NQHET:
%     inp = 0 (provide input file inpf)
%         = 1 (impulse response)
%     npoints = number of points in input
%     w0 = heterodyne frequency
%     [bnq,anq] = coefficients of the Nyquist Filter
%     [b,a] = coefficients of filter H(z)
%
% OUTPUTS: hdb = frequency response of the filter
%          udb, vdb, wdb, ydb
clear y ydb yout hdb u udb v vdb w wdb
if inp==1
    for index=1:npoints
        inpf(index)=0;
    end
    inpf(1)=1;
end
u=filter(bnq,anq,inpf);
for index=1:npoints
    v(index)=u(index)*exp(-1i*w0*(index-1));
end
w=filter(b,a,v);
for index=1:npoints
    y(index)=w(index)*exp(1i*w0*(index-1));
end
udb=20*log10(abs(fft(u)));
vdb=20*log10(abs(fft(v)));
wdb=20*log10(abs(fft(w)));
ydb=20*log10(abs(fft(y)));
yout=2*real(y);
hdb=20*log10(abs(fft(yout)));
plot(hdb,'k')

```

5.3 Example design of nyquist tunable complex heterodyne filter using circuit of Figure 26 (Soderstrand's technique)

The Nyquist Technique is very general and can rotate any type filter, IIR or FIR, low-pass, high-pass, band-pass or band-stop. However, one of the most important uses of the Nyquist Complex Heterodyne Filter is the design of a tunable band-stop filter that can be used to attenuate narrow-band interference in spread-spectrum receivers. To design tunable stop-band filters, the prototype filter, $H(z)$, must be a high-pass filter with cut-off frequency set to one-half the desired bandwidth of the desired tunable band-stop filter. The high-pass prototype filter should have the same stop-band attenuation and pass-band ripple as the desired tunable band-stop filter as all characteristics of the prototype filter are maintained in the tunable filter. The MatLab instruction to design the prototype high-pass filter is

$$a=1;b=firpm(64,[0 0.05 0.15 1],[0 0 1 1],[1 30]);$$

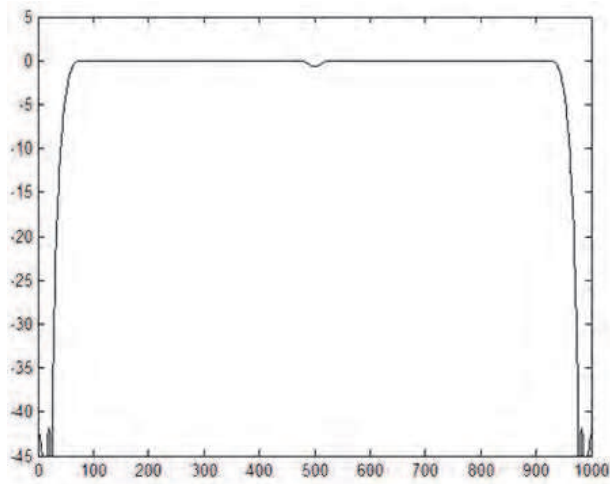
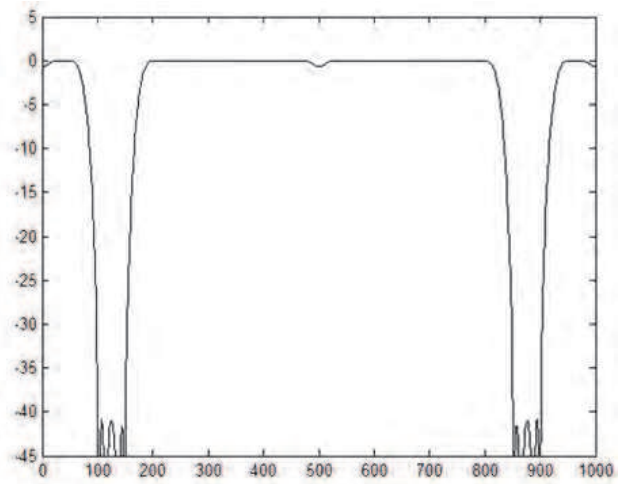
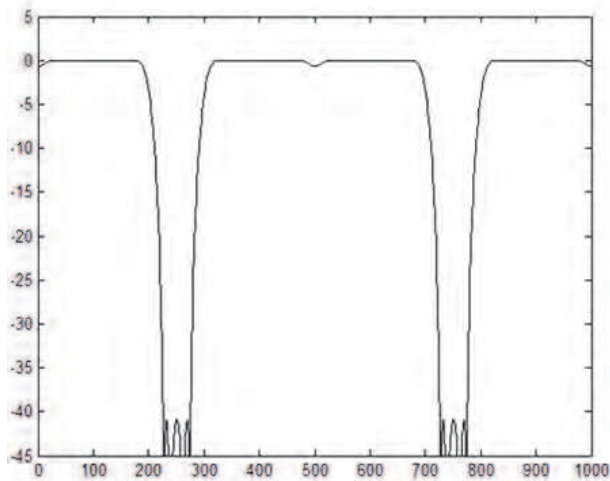
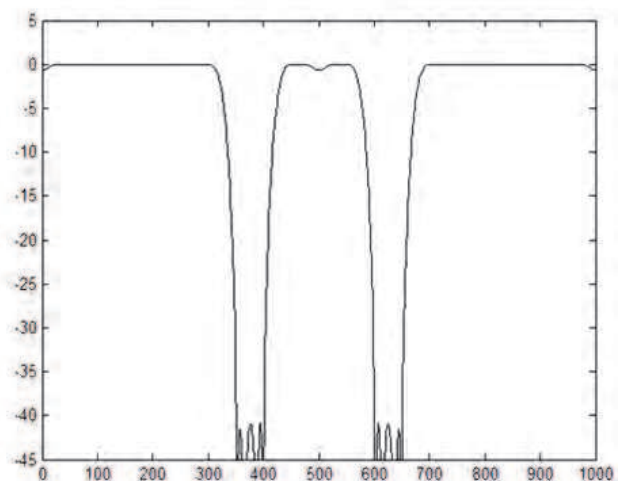
Fig. 28a. Nyquist tunable band-stop $\omega_0 = 0$ Fig. 28b. Nyquist tunable band-stop $\omega_0 = \pi/4$ Fig. 28c. Nyquist tunable band-stop $\omega_0 = \pi/2$ Fig. 28d. Nyquist tunable band-stop $\omega_0 = 3\pi/4$

Fig. 28. Example of nyquist tunable complex heterodyne filter (Soderstrand's technique) for a tunable band-stop filter with 40db attenuation in the stop band, less than .1 db ripple in the pass-band and bandwidth $\pi/10$.

Figure 28 shows the MatLab simulation of the Nyquist Tunable Complex Heterodyne Filter of the circuit of Figure 26. This is fully tunable from DC to the Nyquist frequency. For example, to get the plot of Figure 28d, we use:

```
inp=1;npoints=1000;w0=3*pi/4;nqhet;
```

Notice the dip at DC and the Nyquist Frequency. This is due to the Nyquist Filter not having 3db attenuation at DC. We deliberately allowed the attenuation to be 5db to demonstrate the effect of not having 3db attenuation at DC in the Nyquist filter. However, the effect is negligible only causing a ripple of less than 1db. If the attenuation were greater, the dip would be greater. If the attenuation is less than 3db, we would see a upward bulge at DC and the Nyquist frequency in Figure 27. The tunable filter has the same stop-band

attenuation and pass-band ripple as the prototype filter except for this added ripple due to the Nyquist filter. The bandwidth of the stop-band is twice the bandwidth of the prototype filter.

5.4 Summary of nyquist tunable complex heterodyne filter (Soderstrand's technique)

The Nyquist Complex Heterodyne Technique has the advantage of using the least hardware or software of any of the complex heterodyne filter techniques. The technique is particularly useful in designing full tunable band-stop filters with characteristics identical to the prototype filter but tunable from DC to the Nyquist frequency.

Figure 26 is the basic Nyquist Complex Heterodyne Circuit used to implement these filters in software or hardware. A practical implementation of this circuit has been reported in the literature in a paper appearing in the proceedings of the International System on a Chip Conference (Soderstrand & Cho, 2009). The Nyquist Complex Heterodyne band-stop filters reported in this paper are aimed at narrow-band attenuation in spread-spectrum radio receivers. In section 6 of this chapter we shall show how to make these tunable filters adaptive so that they can automatically vary center frequency, cut-off frequency or bandwidth to adapt to various signal processing needs.

6. Making the tunable filters adaptive

While tunable filters may be of interest in themselves, the primary interest in Tunable Complex Heterodyne Filters is to make them into Adaptive Complex Heterodyne Filters that can automatically detect interference and adapt the tunable filter to the correct place to attenuate the interference. In this section we shall look at how to adapt tunable complex heterodyne band-stop or notch filters to attenuate narrow-band noise in wide-band communication systems such as Frequency Hopping (FHSS) and Direct Sequence Spread Spectrum (DSSS) receivers. This approach is based on a series of papers presented at international conferences (Nelson, et. al., 1997, Soderstrand 2006, 2007, 2010a, 2010b) and two patents (White, et.al. 1999, White, et.al. 2003).

6.1 Narrow-band interference detection circuit

Figure 29 shows the circuit used to make the tunable heterodyne filters into adaptive heterodyne filters. The input $x(n)$ is simultaneously provided to an Attenuation Frequency

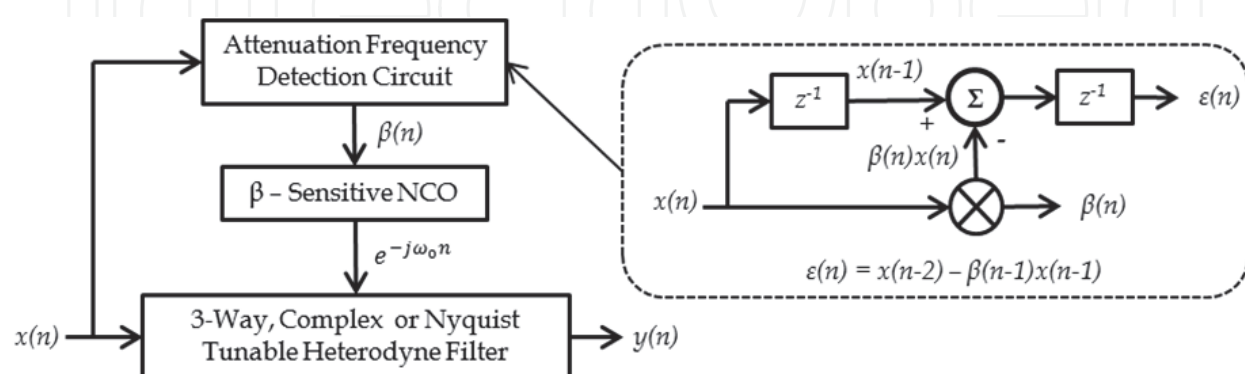


Fig. 29. Narrow-band interference detection circuit to turn tunable complex heterodyne filters into adaptive complex heterodyne filters.

Detection Circuit and to the Tunable Complex Heterodyne Filter. The Attenuation Frequency Detection Circuit (shown in inset) is a simple second-order FIR LMS adaptive notch filter. Because the detection circuit is FIR it will identify the interference without bias. Furthermore, this simple second-order FIR filter is known to be robust and to converge quickly on the correct frequency. However, the simple second-order FIR filter does not provide an adequate attenuator for the narrow-band interference because it attenuates too much of the desired signal. Therefore we only use the detection circuit to determine the value of β needed to generate the complex heterodyne tuning signal $e^{-j\omega_0 n}$. This value of β is fed to a numerically controlled complex oscillator that produces the complex heterodyne signal $e^{-j\omega_0 n}$.

6.2 Comparison of adaptive three-way complex heterodyne band-stop filter to adaptive gray markel lattice

To illustrate the performance of adaptive complex heterodyne filters, we shall set up a simulation in MatLab to compare the performance of the Three-Way Complex Heterodyne Filter to the very popular Gray-Markel Lattice (Gray, 1973, Petraglia, 1994). Figure 30 shows the simulation test setup.

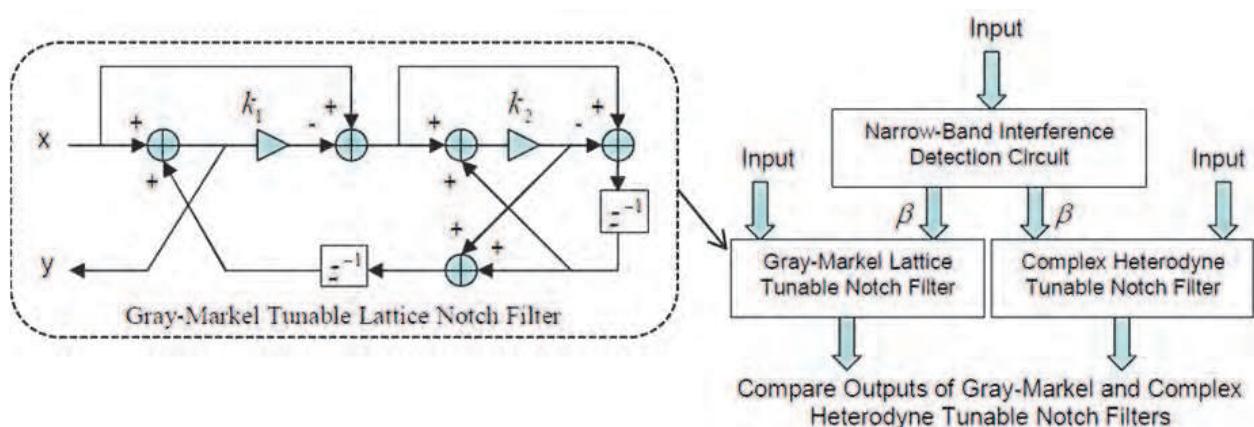


Fig. 30. Test setup for simulation in MatLab of a comparison of adaptive complex heterodyne filters to adaptive gray-markel lattice filters.

Figure 31 shows plots of the energy leakage during a transition of the narrow-band interference from one frequency to another. Both the Gray Markel and the Complex Heterodyne Adaptive Filters track the interference very well. However, in large transitions such as those shown in Figure 31a (transition from frequency $\pi/24$ to $11\pi/24$) and Figure 31b (transition from $\pi/12$ to $5\pi/12$) the Adaptive Complex Heterodyne Filter provides more attenuation of the narrow-band interference than the Gary-Markel Adaptive Filter. In the case of Figure 31a, the difference is about 20db and in the case of Figure 31b it is only about 10db. However, these represent significant differences in the ability to attenuate a fast moving signal. On the smaller transitions of Figure 31c (transition from $\pi/8$ to $3\pi/8$) and Figure 31d. (transition from $\pi/4$ to $\pi/8$) there is little difference between the two filters (although the Gray-Markel adaptive filter is a bit smoother in the transition). The point of this simulation is to show that Adaptive Heterodyne Filters offer an excellent alternative to currently used adaptive filters such as the Gray-Markel adaptive filter.

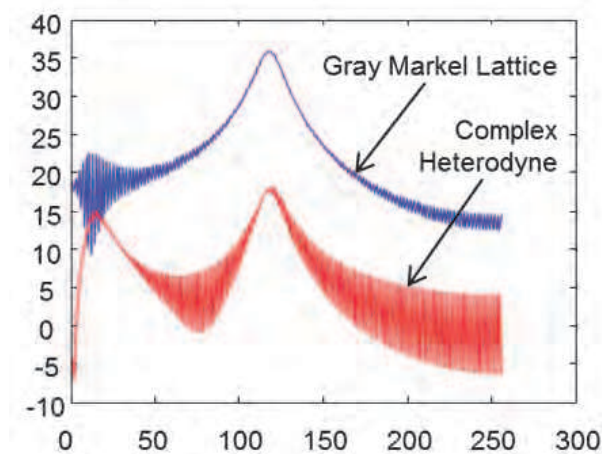
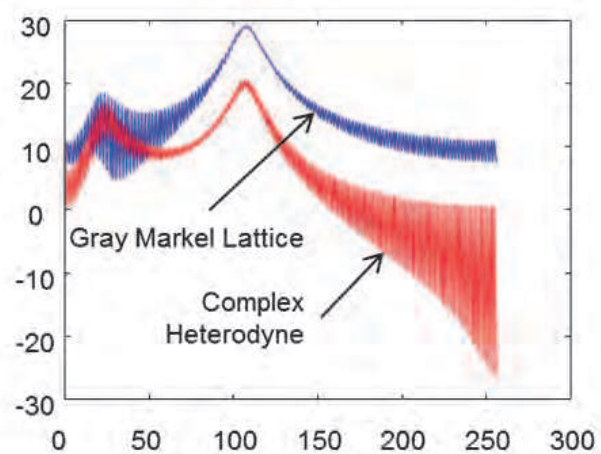
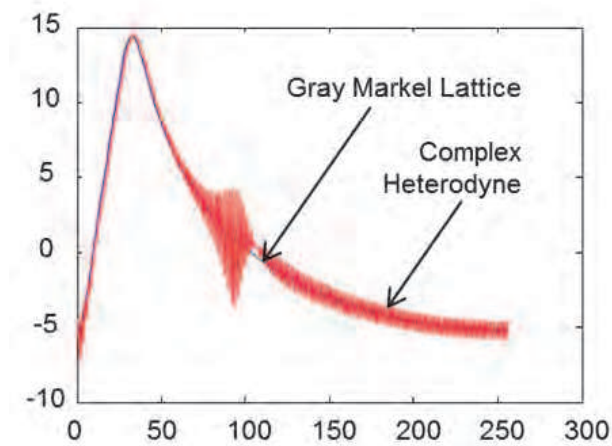
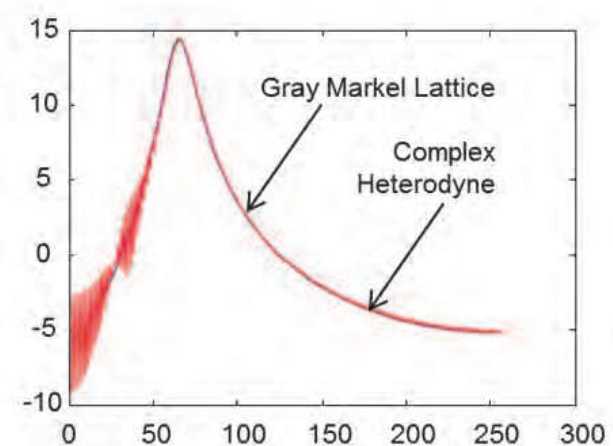
Fig. 31a. Transition from $\pi/24$ to $11\pi/24$ Fig. 31b. Transition from $\pi/12$ to $5\pi/12$ Fig. 31c. Transition from $\pi/8$ to $3\pi/8$ Fig. 31d. Transition from $\pi/4$ to $\pi/8$

Fig. 31. Comparison of gray-markel and complex heterodyne adaptive filters while tracking a moving signal.

7. Summary and conclusions

In this chapter we have explored four techniques for designing tunable filters using a heterodyne signal as the tuning agent:

1. The **Simple Tunable Heterodyne Filter** of Figure 2 requires only two real heterodyne operations, but is limited to tuning the center frequency of narrow-band band-pass filters. However, this is the preferred technique for designing tunable band-pass filters unless the bandwidth of the filter is too large to accommodate the requirements of Figure 2.
2. The **Three-Way Tunable Complex Heterodyne Filter** (Azam's Technique) of Figure 9 requires three complex heterodyne operations, but is able to implement tunable center-frequency band-stop and notch filters, tunable cut-off low-pass and high-pass filter, and tunable bandwidth band-stop and notch filters. However, it is not suitable for tunable center frequency band-pass filters.

3. The **Bottom-Top Tunable Complex Heterodyne Filter** (Cho's Technique) of Figure 21 has all the other tunable heterodyne filters as special cases. This is the most flexible tunable heterodyne filter, but also requires the most hardware.
4. The **Nyquist Tunable Complex Heterodyne Filter** (Soderstrand's Technique) of Figure 26 is ideally suited for implanting center-frequency tunable filters. Center-frequency tunable Band-pass and band-stop filters are most suited to this technique. This technique is able to implement full tunable filters from DC to the Nyquist frequency.

By matching the proper technique above to the particular application it is possible to design extremely efficient tunable filters and then make use of techniques like the one outlined in section 6 to make those tunable filters adaptive. The example of section 6 is typical of what can be accomplished using these new tunable heterodyne filters.

8. References

- Azam, Azad, Dhinesh Sasidaran, Karl Nelson, Gary Ford, Louis Johnson and Michael Soderstrand (2000), Single-Chip Tunable Heterodyne Notch Filters Implemented in FPGA's, *IEEE International Midwest Symposium on Circuits and Systems*, Lansing, MI, August 8-11, 2000.
- Butler, Lloyd, (1989) *Introduction to the Superheterodyne Receiver*, Amateur Radio, March 1989, available from <http://users.tpg.com.au/users/lbutler/Superhet.htm>, accessed 12/11/2010.
- Cho, Grace Yoona, (2005) Louis G. Johnson & Michael A. Soderstrand, New Complex-Arithmetic Heterodyne Filter, *IEEE International Symposium on Circuits and Systems*, vol. 3, pp. 593-596, May, 2005.
- Coulson, A.J. (2004) Narrowband Interference in Pilot Symbol Assisted OFDM Systems, *IEEE Transactions on Wireless Communications*, vol. 3, no. 6, pp. 2277-2287, November 2004.
- Dorf, Richard C. & Zhen, Wan (2000) The z-Transform, In: R.C. Dorf, *The Electrical Engineering Handbook*, CRC Press, available at http://www.4shared.com/document/VA837U3Q/ebook_-_Electrical_Engineering.html, Chapter 8, section 8.2, ISBN 978-0-84-93018-8.
- Duman, Tolga M., (2005) Analog and Digital Communications, In: R.C. Dorf, *The Engineering Handbook*, 2nd Ed, CRC Press, chapter 135, ISBN 0-8493-1586-7.
- Etkin, R, Parekh, A & Tse, D, (2005) Spectrum Sharing for Unlicensed Bands, *Proceedings of the 43rd Allerton Conference on Communications, Control and Computing*, ISBN 978-1-60-423491-6, Monticello, Illinois, September 2005.
- Gray, A.H. Jr., (1973) & John D. Markel, Digital Lattice and Ladder Filter Synthesis, *IEEE Transactions on Audio*, vol. AU-21, no. 6, pp. 491-500, Dec 1973.
- McCune, Earl, (2000) DSSS vs. FHSS Narrowband Interference Performance Issues, *mobile Development and Design*, September 1, 2000, available from http://mobiledevdesign.com/hardware_news/radio_dsss_vs_fhss/
- Nelson, K.E., (1997), P-V.N. Dao, M.A. Soderstrand, S.A. White, J.P. Woodard, A Modified Fixed-Point Computational Gradient Descent Gray-Markel Notch Filter Method for

- Sinusoidal Detection and Attenuation," *IEEE International Symposium on Circuits and Systems, ISCAS '97*, June 9-12, 1997, pp. 2525-2528.
- Peha, Jon M., (1998) Spectrum Management Policy Options, *IEEE Communications Surveys*, vol. 1, no. 1, 4th quarter, 1998.
- Peha, Jon M. (2000) The Path Towards Efficient Coexistence in unlicensed Spectrum, *IEEE 802.16 Wireless High-Speed Unlicensed Metropolitan Area network Standards*, April, 2000.
- Petraglia, Mariane, (1994), Sanjit Mitra & Jacques Szczupak, Adaptive Sinusoid Detection Using IIR Notch Filters and Multirate Techniques, *IEEE Trans CAS - 11*, vol. 41, no. 11, pp. 709-717, Nov 1994.
- Roberts, Michael J. (2007) *Derivation of the Properties of the z-Transform*, Web Appendix O, p. O-3, February 18, 2007, available from <http://www.ece.utk.edu/~roberts/WebAppendices/O-zTransformDerivations.pdf>.
- Soderstrand, Michael A. (2006) Steven R. Phillips, Grace Yoona Cho & David JungPa Lee, Adaptive Notch Filters Using Complex Heterodyne Approach, *IEEE International Midwest Symposium on Circuits and Systems (MWSCAS)*, San Juan Puerto Rico, August 6-9, 2006.
- Soderstrand, Michael A. (2007) & W. Kenneth Jenkins, Comparison of Two Techniques for Attenuation of Narrow-Band Interference in Spread-Spectrum Communications Systems, *IEEE International Midwest Symposium on Circuits and Systems (MWSCAS)*, Montreal, Canada, August 5-8, 2007.
- Soderstrand, Michael A. (2009) & Grace Yoona Cho, A Novel Structure for Tunable Complex Heterodyne Filters, *International System on a Chip Conference (ISOCC)*, Busan, Korea, November, 2009.
- Soderstrand, Michael A. (2010a) Future of Wireless Tutorial, *IEEE International Midwest Symposium on Circuits and Systems (MWSCAS)*, Seattle, WA, August 1-4, 2010..
- Soderstrand, Michael A. (2010b) Noise Reduction Communication Circuits, *International System on a Chip Conference (ISOCC)*, Incheon, Korea, November, 2010.
- White, S.A., (1999) J.P. Woodward, M.A. Soderstrand, K.E. Nelson and P.V.N. Dao, "Adaptive Removal of Resonance Induced Noise", U.S. Patent No. 5960091, Sept. 28, 1999.
- White, S.A., (2003) J.P. Woodward, M.A. Soderstrand, K.E. Nelson and P.V.N. Dao, "Adaptive Removal of Resonance Induced Noise (modified)", U.S. Patent No. 6,011,602, August 26, 2003



Adaptive Filtering

Edited by Dr Lino Garcia

ISBN 978-953-307-158-9

Hard cover, 398 pages

Publisher InTech

Published online 06, September, 2011

Published in print edition September, 2011

Adaptive filtering is useful in any application where the signals or the modeled system vary over time. The configuration of the system and, in particular, the position where the adaptive processor is placed generate different areas or application fields such as prediction, system identification and modeling, equalization, cancellation of interference, etc., which are very important in many disciplines such as control systems, communications, signal processing, acoustics, voice, sound and image, etc. The book consists of noise and echo cancellation, medical applications, communications systems and others hardly joined by their heterogeneity. Each application is a case study with rigor that shows weakness/strength of the method used, assesses its suitability and suggests new forms and areas of use. The problems are becoming increasingly complex and applications must be adapted to solve them. The adaptive filters have proven to be useful in these environments of multiple input/output, variant-time behaviors, and long and complex transfer functions effectively, but fundamentally they still have to evolve. This book is a demonstration of this and a small illustration of everything that is to come.

How to reference

In order to correctly reference this scholarly work, feel free to copy and paste the following:

Michael A. Soderstrand (2011). Adaptive Heterodyne Filters, Adaptive Filtering, Dr Lino Garcia (Ed.), ISBN: 978-953-307-158-9, InTech, Available from: <http://www.intechopen.com/books/adaptive-filtering/adaptive-heterodyne-filters>

INTECH
open science | open minds

InTech Europe

University Campus STeP Ri
Slavka Krautzeka 83/A
51000 Rijeka, Croatia
Phone: +385 (51) 770 447
Fax: +385 (51) 686 166
www.intechopen.com

InTech China

Unit 405, Office Block, Hotel Equatorial Shanghai
No.65, Yan An Road (West), Shanghai, 200040, China
中国上海市延安西路65号上海国际贵都大饭店办公楼405单元
Phone: +86-21-62489820
Fax: +86-21-62489821

© 2011 The Author(s). Licensee IntechOpen. This chapter is distributed under the terms of the [Creative Commons Attribution-NonCommercial-ShareAlike-3.0 License](#), which permits use, distribution and reproduction for non-commercial purposes, provided the original is properly cited and derivative works building on this content are distributed under the same license.

IntechOpen

IntechOpen